

THE RIO APA CRATON IN MATO GROSSO DO SUL (BRAZIL) AND NORTHERN PARAGUAY: GEOCHRONOLOGICAL EVOLUTION, CORRELATIONS AND TECTONIC IMPLICATIONS FOR RODINIA AND GONDWANA

Umberto G. Cordani^{1,*}, Wilson Teixeira¹, Colombo C. G. Tassinari¹, José M. V. Coutinho¹, and Amarildo S. Ruiz²

¹Institute of Geosciences, University of São Paulo, Rua do Lago 562, 05508-080, São Paulo, Brazil.

²Institute of Geosciences, Federal University of Mato Grosso, Cuiabá, Brazil.

*Corresponding author: ucordani@usp.br

ABSTRACT. The Rio Apa cratonic fragment, in the central part of South America, is covered by the Neoproterozoic deposits of the Corumbá and Itapocumi Groups and is bound to the east by the southern portion of the Paraguay-Araguaia belt. It outcrops in Mato Grosso do Sul State of Brazil and in northeastern Paraguay, comprising igneous and metamorphic rocks that can be classified into the following lithotectonic units: (1), the gneissic rocks of the Rio Apa Complex; (2), the intrusive granitic rocks of the Alumiador Suite; (3), the Alto Tererê medium-grade supracrustal rocks; (4), the Caracol orthogneisses; (5), the felsic volcanics of the Serra da Bocaina Group; (6), the gabbro-anorthositic Serra da Alegria Intrusive Suite; (7), the Amolar low-grade metasedimentary rocks; (8), the granitic, gneissic and migmatitic rocks of the Paso Bravo Province in Paraguay.

In this work, the available radiometric ages and isotopic determinations were reassessed in order to achieve a complete picture of the regional geological history. More than 100 age and isotopic results were discussed, including U-Pb SHRIMP ages in zircons, Rb-Sr and Sm-Nd whole-rock determinations, and K-Ar and Ar-Ar mineral ages. Taking into account the available data, the tectonic evolution of the Rio Apa Craton rocks seems to be related to a series of magmatic arc complexes, whose original magmas involve some crustal component. For all the lithotectonic units, the Sm-Nd T_{DM} model ages were roughly between 2.0 Ga and 2.50 Ga, as a response from the nature of the original material and the particular characteristics of crustal evolution. A gneissic rock from the northern part of the region yielded a U-Pb zircon age of 1940 Ma. Gneissic rocks similarly occur at the western part of the region and are intruded by the Alumiador Suite, from which two monzogranites yielded U-Pb zircon ages of about 1850 Ma. Overlying the western area, the felsic volcanics of the Serra da Bocaina Group yielded a U-Pb zircon age of 1790 Ma. A similar U-Pb age was obtained from an anorthosite from the magmatic suite of the Serra da Alegria. To the east-southeast of this area the Caracol orthogneisses give ages between 1760 and 1700 Ma. They may be coeval with the Alto Tererê metamorphics, to the north, which are intruded by granitoids at that time. A widespread regional Sr isotopic homogenization, associated with medium-grade metamorphism and deformation occurred at about 1680 Ma, as suggested by several reference-whole rock isochron ages. Finally, near 1300 Ma ago, the Rio Apa Craton was affected by a widespread regional heating, when the temperature for the region probably surpassed 350°C.

The geographic distribution, age and isotopic signature of the lithotectonic units, together with the available geologic information, permit a speculation for the existence of a major transcurrent or transpressional fault zone separating two different tectonic domains that were juxtaposed at the time in which the principal regional deformation affected the entire area, at 1680 Ma. From that time on, the unified Rio Apa block behave as one singular and tectonically stable cratonic mass. Regarding tectonic correlations, the Rio Apa cratonic fragment correlates well with the SW corner of the Amazonian Craton, where the granitic and gneissic rocks of the Juruena-Rio Negro tectonic province, with ages between 1600 and 1780 Ma, are reworked by tectonic events related with the younger, adjacent Rondonian-San Ignacio province, exhibiting a strong metamorphic imprint at about 1300 Ma. It could also be compared strictly with the Paraguá block, within the Rondonian-San Ignacio Province, where basement inliers with 1600-1800 Ma are found. Looking at a larger scale, a complex arrangement of allochthonous blocks with different sizes is seen as a consequence of the repeated interaction between Laurentia and Amazonia during the entire Proterozoic. They may have been trapped during the collisions of the two main continental masses, and may have originated as disrupted parts of either Laurentia or Amazonia, or accretionary terranes newly formed within an intervening ocean. In other words the Rio Apa and Paraguá blocks may be relicts of such geodynamic processes likewise analogous terranes such as Arequipa, Antofalla and Pampia.

Keywords: Rio Apa Craton, geochronology, South America, tectonic evolution, geotectonic correlations

INTRODUCTION

The Rio Apa cratonic fragment, in the central part of South America (fig. 1 and 2), 220 km long x 60 km wide, is poorly exposed, being covered by extensive Phanerozoic sedimentary sequences. It crops out at the Brazilian border with Bolivia and Paraguay and extends to the south into Paraguayan territory. It is part of a tectonically stable cratonic domain for the Paraguay-Araguaia belt, folded and regionally metamorphosed during the Neoproterozoic Brasiliano Orogeny, and it is overlain by the mainly carbonatic platform covers of the Corumbá and Itapocumi Groups (Almeida, 1965, 1967; Alvarenga and others, 2000).

Almeida (1967) was the first to suggest that the Rio Apa region was a direct link of his "Guaporé Craton", which is the southern part of what is now named "Amazonian Craton". When we consider the geotectonic setting of southern South America for Neoproterozoic time, two main scenarios, among others, must be considered in relation to the Rio Apa cratonic fragment. One of them, proposed by several authors, among which Dell'Arco and others (1982), Alvarenga and Saes (1992), Kroener and Cordani (2003) and others, envisage the Rio Apa as an allochthonous feature, which during the agglutination of Gondwana was attached to the Amazonian Craton along the Neoproterozoic Tucavaca belt, considered as a suture. This scenario is illustrated by figure 1, taken from Kroener and Cordani (2003). The other, proposed by Ruiz and others (2003), and followed among others by Cordani and others (2009), envisaged the Rio Apa cratonic fragment as a prolongation of the Amazonian Craton, in the Neoproterozoic. In this case the Tucavaca belt would correspond to an aulacogenic feature, developed over a continental

crust as a reflection of the compressional tectonic episodes of the Paraguay-Araguaia orogen. Figure 2, adapted from Ruiz and others (2003) illustrates this idea.

Figure 1 – Adapted from Kroener and Cordani, 2003.

Figure 2 – Adapted from Ruiz and others, 2005.

The position of the Rio Apa cratonic fragment within the context of the Meso and Neoproterozoic supercontinents, and consequently its correlation with its neighbouring continental masses, is relevant in order to investigate the tectonic evolution of the Grenvillian-type age mobile belts related to the agglutination of Rodinia and Gondwana. For the terminal Mesoproterozoic time, the correlation must be attempted taking into account the tectonic provinces of the Amazonian Craton, as well as the very dispersed Grenvillian-type age basement inliers within the younger tectonic framework of the Andean Cordillera. Therefore, the determination of its geologic history is crucial to put on a better basis its possible past position within the context of Rodinia. In addition, it is also important in order to suggest its role during the agglutination of Gondwana.

A great deal of geochronological work for the Rio Apa cratonic fragment was already available, since the first comprehensive geological mapping efforts (Araujo and others, 1982; Godoi and others, 1999), in which several Rb-Sr and K-Ar determinations were obtained at a reconnaissance scale. As a result of these initiatives, the polymetamorphic character of the region was already clearly demonstrated, and it was enhanced by the more recent works (Lacerda-Filho and others, 2004; Cordani and others, 2005; Cordani and Teixeira, 2007), when a few Sm-Nd and Ar-Ar were added to the existent data, as well as some U-Pb SHRIMP determinations. This important assemblage of geochronological data makes possible to compare and evaluate the interpretative values of different dating methods, employed often in the same rock samples, collected within the same area, and belonging to the same geological context.

Therefore, the objective of this work is threefold:

1. To integrate the interpretation of the geochronological data in order to establish the relative sequence of the regional tectonic events.
2. To make an attempt to establish the tectonic significance of the apparent ages and isotopic constraints, as determined by different methods.
3. To make an attempt to correlate the Rio Apa cratonic fragment, with the neighbouring tectonic provinces within central South America, in order to propose a suitable relative position of it in Rodinia and Gondwana.

GEOLOGICAL SETTING

Figure 3 brings a reconnaissance map of the main area of exposure of the Rio Apa Craton, bounded to the east by the Paraguay-Araguaia belt, in SW Mato Grosso do Sul and northeastern Paraguay. This figure was compiled after a re-examination of the previous geological maps at the Brazilian side, produced by Araujo and others (1982) and Godoy and others (1999), and was adapted following as much as possible the 1:1000000 digital geologic maps published by Delgado and others (2003) and Lacerda Filho and others (2004), where the previous information was already considered. For the territory of Paraguay, the main information was taken from the reconnaissance geological map produced by the Anchutz Corporation in the 80's, later

incorporated by Fernando Wiens in his PhD dissertation (Wiens, 1986). In addition, the observations of the senior author, made during a short trip to the area in 2003, when the samples used in this study were collected, were also taken into consideration.

Figure 3 – Geologic map

In this work, the recent sediments of the Pantanal Formation and the sedimentary rocks of the Aquidauana Formation, which cover extensive areas in figure 3, will not be discussed. Also the Fecho dos Morros alkaline complex, of Triassic age, will not be dealt with. For the Precambrian units, the interpretation of its geological history, and especially its structural evolution, is very complicated. To give some immediate information, useful for the understanding of the regional geological history, the available U-Pb SHRIMP zircon ages listed in Appendix 2 are highlighted in figure 3. As will be considered later, when dealing with the geochronological interpretation, they were obtained from magmatic rocks or orthometamorphic rocks.

Looking at the geotectonic setting displayed in both figures 1 and 2, the Rio Apa Craton is the stable tectonic domain for the Neoproterozoic Paraguay-Araguaia belt. The Rio Apa basement rocks are overlain along the Serra de Bodoquena in Brazil, and at the southernmost part of the region, in Paraguay, by the intracratonic covers of the Corumbá Group (in Brazil) and Itapocumi Group (in Paraguay). In these sequences carbonatic sediments predominate, displaying a fossiliferous content (Claudina, Corumbella) indicating their age close to the Precambrian-Cambrian boundary (Boggiani and others, 1993). The Corumbá Group exhibits a clear tectonic and metamorphic polarity increasing toward the easternmost part of the region, where the low-grade metasedimentary rocks of the Paraguay-Araguaia belt occur, as a tectonic feature of the Neoproterozoic Brasiliano Orogeny. Figure 3 includes, in its north-eastern corner, the low to medium-grade metamorphic rocks of the Cuiabá Group, predominantly muscovite schists and quartzites, which exhibit NW-SE trending conspicuous structures. These correspond to large fault zones, in which the Cuiabá fold and thrust belt overrides the less metamorphic sequences of the Corumbá Group.

Description of the Lithological Units of the Rio Apa Craton

In the northern part of the basement area, banded gneisses and migmatites predominate, with frequent intercalations of amphibolite. One of these hornblende-biotite gneiss yielded a well confirmed U-Pb SHRIMP age near 1940 Ma (fig. 3). These medium to high grade metamorphic rocks were included by Lacerda Filho and others (2004) in their Rio Apa Complex, and were attributed to a series of Paleoproterozoic magmatic arcs.

Adjacent to the Rio Apa Complex in the northern area, a sequence of low to medium grade metavolcano-sedimentary rocks occur, where muscovite-biotite schists are the predominant rocks, sometimes with garnet porphyroblasts, but muscovite-biotite gneisses and quartzite intercalations are frequent, and metabasic rocks are also indicated in many places. The differential erosion between the schists and the large quartzite intercalations enhance the complicated sinuous structures, shown in figure 3, that further indicate the complexity of the structural regional context of the Alto Tererê metamorphic terrain. This tectonic unit was named Alto Tererê association by Corrêa and others (1976), and the name was retained by Godoi and others (1999) and Lacerda Filho and others (2004). In the northeastern part of the area, between the towns of Morraria and Baía das Garças, the Alto Tererê schists are intruded by slightly

foliated granitoid rocks, dated by SHRIMP at about 1730 Ma (Appendix 2), and forming three small areas located very close to the contact with the overlying Corumbá Group.

To the east of the town of Porto Murtinho, banded gneissic rocks occur, covered by the felsic volcanics of the Serra da Bocaina Group, and intruded by the granitoid rocks of the Alumiador Suite (Araujo and others, 1982). These basement rocks are considered by Lacerda Filho and others (2004) as possibly correlative with the northern gneisses of the Rio Apa Complex, and some xenoliths of them are observed within the Alumiador batholith. This large granitic intrusion takes the form of an elongated batholith in the central part of the region, showing conspicuous lineaments trending NNE-SSW along the Serra do Alumiador, and deflecting to NW-SE trends along the Serra da Alegria. They are formed essentially by fine to medium grained isotropic syeno to monzogranites, also including some granophyric varieties. Two U-Pb SHRIMP ages, location shown in figure 3, indicate an average age near 1850 Ma for the Alumiador granite in its southern part. The second large portion of the Alumiador suite forms an extension to the north, trending NW-SE and including similar granitic rocks. In this region, the batholith is surrounded and intruded by the gabbro-anorthositic suite named Serra da Alegria, as reported by Silva (1998), and retained by Lacerda Filho and others (2004). It is a cumulatic magmatic suite, in which anorthosites, and leuco-gabbros to mela-gabbros are described, some of them with igneous banding. A U-Pb SHRIMP zircon age of 1790 Ma was obtained from an anorthosite (fig. 3). The gabbroic rocks of the Triunfo Mafic Complex, indicated in figure 3, from which a suitable age is not yet available, may be correlative with the Serra da Alegria magmatic rocks. Mainly because of the lack of geochronological control, in all works related to regional mapping (Araujo and others, 1982; Godoy and others, 1999; Delgado and others, 2003; Lacerda Filho and others, 2004, among others), all intrusive granitoid bodies occurring in the region were considered correlative with the Alumiador granitic suite. This is the case, for example, of the granites associated to the Alto Tererê Group in the northeast corner, near Baía das Garças, and also of the granitic rocks located near the Apa River, that intrude the Amolar meta-sedimentary domain.

The volcanic rocks of the Serra da Bocaina Group include porphyritic rhyolites and dacites, associated with minor pyroclastics and volcanic breccias. A rhyolite occurring in the northern part, close to the Serra da Alegria, and considered correlative to the main Serra da Bocaina volcanics of Porto Murtinho, yielded a U-Pb SHRIMP age of 1794 Ma. To Araujo and others (1982) and also by most subsequent authors, the volcanics have been considered to be the extrusive equivalents of the Alumiador granites.

In the central part of the region, from about the latitude of the town of Bonito, and extending to the south to include the towns of Caracol in Brazil and San Carlos in Paraguay, slightly foliated homogeneous orthogneisses are widespread. They are different from the Rio Apa banded gneisses of the north, and also from the Alumiador granites, especially by their paragenesis, which includes very little amounts of mafic minerals. The mineralogy of all of these leucocratic gneisses is very simple, with quartz, microcline, oligoclase as main components. These rocks were included within the Rio Apa Complex by Lacerda Filho and others (2004), following the previous work by Araujo and others (1982) and Godoi and others (1999). However, because of the much younger U-Pb SHRIMP zircon ages of about 1730 Ma obtained from two of these rocks (fig. 3), they may constitute a different tectonic unit, which will be informally named, in this work, Caracol leucocratic gneisses.

Several outcrops of low to medium-grade metamorphic sequences occurring in the Brazilian part of the region of figure 3 were united by Lacerda Filho and others (2004) under the informal name of "Amolar Domain". They are considered as correlative of the Sunsás orogen (see fig. 1),

and therefore are tentatively attributed to the Mesoproterozoic. The larger area occupied by this unit is identified near the Apa river, forming a large zig-zag structure connecting both sides of the Brazil-Paraguay border. The main lithologies include different types of supracrustal rocks, among which quartzites and sericite-schists predominate. Meta-volcanic rocks are also present, especially in Paraguay. The rocks of the Amolar domain are intruded, in Brazil and Paraguay, by small granitoid plutons. No dating is available yet either from the supracrustal rocks or from the intrusive granites, therefore any possibility of correlation is only tentative.

In the territory of Paraguay, the geological setting is known only at reconnaissance level Wiens (1986). In figure 3 we made an attempt of re-interpreting Wiens's map, making the possible correlations with the work of Lacerda Filho and others (2004). In this respect, at the eastern part of the Paraguayan region, the continuation of the sedimentary rocks of the Paraná Basin is obvious, as well as the correlation of a few small outcrops of limestone with the Corumbá Group. At the western part, the Quaternary cover along the Paraguay river is the same in both countries, and the supracrustal rocks of the Amolar domain form a coherent structure. These low-grade metamorphic rocks are covered by the Itapocumi stromatolitic limestone, in which minor intercalations of siliciclastic rocks occur, and are considered correlative of the Corumbá Group.

To the east of that area, Wiens (1986) described what he included in his Paso Bravo Province, a complex and diversified region in which medium grade metamorphic rocks are predominantly exposed. From his lithological descriptions, we could infer that the western part of that unit, formed by pink to grey, medium to coarse, strongly foliated granitic gneisses, may easily be correlated with the Caracol leucocratic gneisses described above for the Brazilian portion of the Rio Apa Craton. These units are tentatively linked in the geological map of figure 3. On the other hand, the eastern part of the Wiens' (1986) Paso Bravo Province seems not to have a counterpart in Brazil. In that area banded gneisses predominate in which, besides feldspars and quartz, a great deal of mafic minerals is recorded, such as hornblende, biotite, garnet and pyroxene. Migmatites are also described, as well as a few granitic intrusions, formed mainly by medium to coarse biotite granites, massive to weakly foliated, sometimes with muscovite, and locally exhibiting porphyroid texture. In figure 3, this area keeps Wiens' (1986) name of Paso Bravo Province. Unfortunately, the two attempts to obtain U-Pb SHRIMP ages from these rocks failed because of the highly metamict status of their zircons.

Structural Context

Taking into account the many observations made at the available outcrops, by different authors (for example Araujo and others, 1982; Godoi and others, 1999; Lacerda Filho and others, 2004; Ruiz and others, 2005; Godoy and others, 2009), plus those of the present authors, and looking at the available SLAR images taken in the 70's, and also in the more recent satellite imageries, in order to recognize the large-scale regional structures, some general ideas on the regional structural evolution can be made as follows:

1. As expected, the areas covered by the Quaternary formations, as well as by the sedimentary rocks of the Aquidauana Formation and the Corumbá Group are virtually structureless. This also occurs for the peneplanized areas of the various granitoid-gneissic terrains in Brazil and Paraguay. Some low crustal level faults, produced by relatively young Phanerozoic tectonics, are seen affecting the Corumbá and Itapocumi limestones, mainly normal, but sometimes compressional. Moreover, it is apparent that the Nabieleque lowlands, among other swampy terrains, are now subsiding, characterizing one of the

- initial episodes for the formation of a new large sedimentary basin in central South America.
2. Neoproterozoic tectonics, related to the activity of the Paraguay folded belt, is also at low crustal level. The tectonic polarity of the low-grade metamorphic rocks of the Cuiabá Group towards the cratonic area is evident. Recumbent folds are observed, and the rocks exhibit slate cleavage and axial plane schistosity. Later deformational phases are also observed, producing crenulation and mylonitic foliation along transpressive zones. For the platform cover of the Corumbá Group, only gentle folding occurs, with eastward dips and practically vertical axial planes. The same occurs for the Itapocumi Group in Paraguay, but the gentle dips of this unit are westward directed. Moreover, affecting the Puerto Valle-mi outcrop of limestones and shales of the Itapocumi Group, along the Paraguay River, Campanha and others (2008) described a series of thrust faults associated with low-grade metamorphism. Regarding the Rio Apa craton rocks, evidence for the Neoproterozoic tectonics is barely visible.
 3. Considering the basement rocks, a regional foliation seems to be affecting all the lithological units, especially in the southern part of the area. For the Caracol leucocratic gneisses, it stands up as a penetrative schistosity, normally with variable attitudes, possibly related to a pervasive medium-grade metamorphic event. Along the BR 267 road, these rocks show low dipping angles (around 20°) to the SW. In contrast, for the Alumiador suite, a few km to the west, what could be the same structural deformation is observed, exhibiting similar trend but with high dipping angles ($70-80^{\circ}$) always towards SW. For the Serra da Bocaina volcanics, a slaty cleavage is described with moderate dips to the SW that may also be related to the same regional deformation.
 4. A strong deformational episode is recovered also the central and northern areas, where the Rio Apa gneisses and the Alto Tererê schists occur. These units exhibit variable lithologies, with quite different rheological properties, and also variable structural trends. Often at least one older deformational phase is detected. Moreover, the strong penetrative and axial plane schistosity, where this can be observed, is practically parallel to bedding, indicating the existence of isoclinal folding.
 5. It is difficult to include the small and sparse outcrops of low-grade supracrustal rocks occurring in the northwestern part of the region, included by Lacerda Filho and others (2004) in the Amolar domain, in a coherent structural picture. This is only possible for the southern structure that crosses the Rio Apa from Brazil to Paraguay. In Brazil, this structure exhibits NE-SW trend, making up what it seems to be an antiform, with an inverted flank and axial plane dipping towards south-east, whose nucleus is occupied by small granitic bodies (fig. 3). In Paraguay, the same antiform bands sharply to a NW-SE trend, and comes back later to a NE-SW trend, but keeping its eastern dip, and its internal granites. One of these, a biotite granite, forms a nucleus of what Wiens (1986) characterized as “Centurion structural high”. This large “zig-zag” antiform indicates a westward tectonic transport.

GEOCHRONOLOGICAL RESULTS

Age determinations for the Rio Apa Craton were performed essentially at the Geochronology Research Center of the University of São Paulo, firstly for the RADAM Project (Araujo and others, 1982) and more recent for this work, from the samples collected in 2003 by the senior

author. Preliminary informations were presented at a few scientific meetings (Cordani and others, 2005, Cordani and others, 2008a, 2008b). The abstracts given in these events are mentioned in the section on references. All available geochronological data for the region, obtained at the CPGeo-USP or elsewhere, will be presented accordingly with the methodology employed and will be examined and evaluated in terms of the direct interpretative value of each method. Appendix 1 presents the analytical methods, and the results are given in tables 2 to 5, and in appendixes 2 and 3.

U-Pb SHRIMP Determinations

Zircons were extracted from eight samples of granitoid rocks, and dated by the U-Pb SHRIMP method. Appendix 2 brings the complete analytical data, together with four others, reported by Lacerda Filho and others (2004), whose analyses were performed at the Australian National University, Canberra. For the latter, the analytical data, zircon images and Concordia plots are not available. The location of the twelve samples dated is indicated in the geological map of figure 3. The zircon typologies for the samples prepared at the CPGeo-USP are described below, and the Concordia plots for the analytical points are shown in figure 4.

Figure 4 – Concordia diagrams

Sample RA 23, from the northernmost part of the area, is a strongly foliated medium-grade biotite-hornblende gneiss belonging to the Rio Apa Complex, in which plagioclase (45%) predominates over microcline (15%). It also includes quartz (25%), biotite (10%) and hornblende (5%), plus sphene, apatite and epidote. Zircons are mainly subhedral prismatic crystals, 200-300 μm long, with dark oscillatory-zoned cores and small white low-U rims in the CL images. Appendix 2 indicates U content of 200-500 ppm, as well as quite low common Pb correction (Appendix 2). In figure 4A, the three most concordant zircons yielded 1935 ± 15 Ma. The other discordant zircons are disposed along a poorly defined discordia, but tending to an apparent Neoproterozoic episode of Pb-loss. Sample GMR-27, reported by Lacerda Filho and others (2004) comes almost certainly from the same outcrop, according with GPS data, and yielded a very similar U-Pb SHRIMP age.

Sample RA 77 is a pink unfoliated monzogranite of the Alumiador Suite. Its mineral composition includes plagioclase, microcline and quartz in similar amounts, around 30%, plus biotite (less than 10%), sphene, zircon, epidote, apatite and opaques. Texture is equigranular, magmatic-type, with millimetric grain size, but including some centimeter-size K-feldspar crystals. In this sample, large euhedral to subhedral prismatic zircon crystals, 180-300 μm long, are found. CL images show oscillatory-zoned cores and dark (possibly magmatic) resorbed borders. The crystals are dark brown, fractured, and showing filling with high-U zircon. Appendix 2 shows that U content is variable, usually within 70-270 ppm, but with some high-U crystals, up to 800 ppm. In figure 4B, four concordant crystals yielded a mean age of 1829 ± 21 Ma, whilst several discordant zircons are aligned along a poorly defined discordia. Sample CC-09, reported by Lacerda Filho and others (2004), was collected very close to sample RA 77, from the same rock unit (see fig. 3), and was referred as a porphyritic granite. The indicated U-Pb SHRIMP age was 1867 Ma, but experimental error was not reported.

Samples RA 35 and RA 40, collected near Baía das Garças, are unfoliated to slightly foliated, pink coloured granitoid rocks, with very similar mineral composition and textures, which intrude the Alto Tererê metamorphics. They comprise plagioclase (40 to 50%), microcline (about 30 %), quartz (20 to 30 %) and some biotite. Zircon, allanite, apatite, chlorite and opaques are the common accessories. These rocks exhibit medium grain size, millimetric, and magmatic textures. Sample RA 35 consists of euhedral zircon crystals, usually short prisms with pyramid terminations, 50-150 μm long, together with a smaller population of larger crystals, up to 300 μm long. In the CL images oscillatory-zoned cores and relatively large dark overgrowths of high-U zircon are observed. U content is between 250-550 ppm (Appendix 2), but some zircons show high content, up to 2000 ppm. In figure 4C two nearly concordant zircons yielded an age close to 1730 Ma, and the other discordant zircons seem to indicate a multi-branched pattern of Pb-loss. In sample RA 40, zircons are mainly large subhedral crystals, with pyramidal terminations, 200-300 μm long. They are dark brown, and heavy fractured. The CL images are complex, showing oscillatory-zones but also some sector-zoned cores, together with many oscillatory-zoned overgrowths. Small dark rims are observed, as well as embayments filled with high-U zircon. The dated zircons showed moderate U content of 110-320 ppm, and usually low common Pb correction (Appendix 2). In figure 4D, two concordant zircons indicate an age of 1752 ± 46 Ma, and many other discordant zircons exhibit large scattering along split discordias, generated by effects of multi-stage Pb-loss. In general, they seem to bear a tendency to a Neoproterozoic lower intercept.

Samples RA 81 and RA 84, collected near Caracol, are slightly to moderately foliated medium to high-grade leucocratic orthogneisses, light grey to pink, with very similar mineral composition. They comprise microcline (30-40 %), quartz (35-40%), plagioclase (20-25%), and some biotite (usually less than 5 %). Zircon, apatite, epidote and opaques are the common accessories. These rocks exhibit medium grain size, and textures are always granoblastic. Sample RA 81 includes a population of subhedral to euhedral prismatic zircons, 80-200 μm long, some rounded and exhibiting resorption features. CL images show complex structures, with cores of different types as well as borders and embayments with high-U filling. The U content is very variable, usually between 150-900 ppm (Appendix 2). One zircon crystal had more than 2000 ppm. Figure 4E shows that the two most concordant plots yielded $^{207}\text{Pb}/^{206}\text{Pb}$ ages of about 1750 Ma. Many discordant zircons were scattered along different discordias resulting from multi-stage Pb-loss. In addition, one concordant crystal showed a much younger age, of 540 Ma, suggesting the possibility of some growth of new zircon during the Neoproterozoic. Sample RA 84 presents subhedral to anhedral short prisms, 80-150 μm long. The CL images show light grey cores with igneous zoning and white low-U rims. Appendix 2 indicates U content between 100 and 200 ppm, and usually low common Pb corrections. Figure 4F shows that practically all measured crystals are concordant or slightly discordant, with an average age of 1721 ± 26 Ma.

Samples RA 95 and RA 111, from Paraguay, are assigned to the Paso Bravo Province of Wiens (1986). The former is a grey granitoid gneiss, and the second is a pink granite. Both rocks are slightly foliated, and are constituted by microcline (about 40%), quartz (35 %) and plagioclase (25%), with minor amounts of biotite, and zircon, apatite, chlorite and opaques as accessories. Sample RA 95 presents large fragments of anhedral crystals, 150-350 μm long, many of them rounded and with evidence of resorption. The CL images show complex structures, in which cores are in part sector-zoned metamorphic-type, and in part made up by magmatic oscillatory-zoned zircon. The crystals have dark borders and many embayments and fractures filled with high-U zircon. The U contents are usually high, some grains with 200-420

ppm, some with 1100-1400 ppm, and several with more than 2200 ppm (Appendix 2). In several cases a large common Pb correction was necessary. Sample RA 111 presents anhedral crystals and fragments, mainly 100-220 μm long, very similar to those of sample 95. Most of them are completely dark, with embayments indicating resorption and metamorphic replacement. Like in sample RA 95, U content of the crystals is usually very large, with at least 900 ppm, and some grains with up to 2800 ppm (Appendix 2). Figures 4G and 4H show that all crystals from both samples are discordant, scattered along split discordias and showing multi-stage Pb diffusion, dominated by recent Pb-loss. Moreover, in both figures, many crystals are relatively close to Concordia for the 1000-1200 Ma interval.

Appendix 2 includes two other U-Pb results reported in Lacerda Filho and others (2004). One of them (JV 14) comes from an anorthosite rock unit belonging to the gabbro-anorthosite suite of the Serra de Alegria, which yielded an age of 1791 Ma. The other relates to a felsic volcanic rock (JV 31) attributed to the Serra da Bocaina Group, which yielded a similar age of 1794 Ma.

In summary, with the exception of samples 95 and 111 (fig. 4G and H), in which all analysed zircon crystals were variably discordant, the other six samples (fig. 4A to F) included at least two concordant or nearly concordant points, making possible the conventional interpretation and relating the preferred $^{207}\text{Pb}/^{206}\text{Pb}$ ages to the main episodes of magmatic crystallization of their protoliths. Moreover, considering the existence of a great majority of discordant crystals, and especially the complex multi-stage pattern displayed by the discordias, it may be suggested that a series of thermal episodes affected the region, and consequently Pb loss may have occurred at different times.

Therefore, for samples RA 23 and RA 77, the few concordant grains allow to interpret their age in the conventional way. The age of the former, 1935 ± 15 Ma, calculated considering the mean of all measured $^{207}\text{Pb}/^{206}\text{Pb}$ analyses, is the first indication for the existence of a Paleoproterozoic magmatic arc in the evolution of the Rio Apa Craton. On the other hand, the age of sample RA 77, 1829 ± 21 Ma, calculated as a mean of seven $^{207}\text{Pb}/^{206}\text{Pb}$ analyses of the most concordant points, represents the intrusive event of the Alumiador Suite. In both cases, a few discordant points indicate the incidence of lead loss during later episodes of the tectonic evolution. Considering the Caracol leucocratic orthogneisses of the central-southern region, only for sample RA 84 a clear indication is given for the age of its protolith, at 1721 ± 26 Ma, calculated as the mean of all seven available $^{207}\text{Pb}/^{206}\text{Pb}$ analyses. However, a good indication is also given by sample RA 81, where a small cluster of near concordant analyses is observed, and an age close to 1760 Ma is determined taken into account the three most concordant ones. Samples RA 35A and RA 40 are of granitoid rocks collected in the vicinity of Baía das Garças town, intrusive into the Alto Tererê meta-sedimentary rocks. For the former an age of ca.1730 Ma is indicated by two nearly concordant points, and the two most concordant points for the second indicated an age close to 1750 Ma. Finally, the analytical points of the two southernmost samples, RA 95 and RA 111, assigned to the Paso Bravo Province, are extremely discordant, precluding the definition of a reliable upper intercept.

The overall number of analysed zircons is not sufficient for a statistical approach; however, looking carefully at all the diagrams, especially those of samples 40, 81, 95 and 111, the scattering about the discordia trends appears to be dominated by recent Pb-loss, especially in the case of the latter two, as a consequence of alteration over metamict zircon crystals. However, there is also some evidence of possible specific Pb-loss episodes related to regional thermal and/or metamorphic episodes. For instance, looking at the $^{206}\text{Pb}/^{238}\text{U}$ ages of Appendix 2, samples RA 40 and RA 95 produced a small cluster of apparent ages between 1100 and 1200

Ma, and sample RA 111 contains some grains with about 1000 Ma. In a general way, for all of the six dated samples, the scatter of the discordant points in the Concordia diagrams does not indicate a unique trend, but a multi-branched pattern of Pb diffusion, achieved by successive Pb-loss episodes, accompanied by recent Pb loss.

Rb-Sr Determinations

Fifty two Rb-Sr whole-rock analyses are now available from rocks of the Rio Apa region, whose location is shown in figure 5. A few of them were obtained in felsic volcanic rocks, but the great majority was performed in granitoid and gneissic rocks. Table 2 brings the analytical data used for the preparation of figure 6, and also includes the calculated Rb-Sr age, assuming a $^{87}\text{Sr}/^{86}\text{Sr}$ initial ratio of 0.705, for those samples with high $^{87}\text{Rb}/^{86}\text{Sr}$ ratio, above 4.0, that shall be meagerly affected by possible differences from their real Sr initial ratios.

Figure 5 – Location of samples analysed by Rb-Sr and Sm-Nd methods

Because they were collected in different outcrops, the samples cannot be considered cogenetic material. Therefore, the best-fit lines calculated from any of the attempted regressions are not real isochrones, and the calculated ages can only be used as a reference. Nevertheless, in an exercise in which all the 52 analytical points were plotted in the same Rb-Sr isochron diagram, with a few exceptions they showed up remarkably aligned. The calculated best-fit line exhibited a slope that would correspond to a reference isochron of about 1700 Ma, with a $^{87}\text{Sr}/^{86}\text{Sr}$ initial ratio of about 0.706. Cordani and others (2005) had already discussed this surprising outcome, giving the large area involved and the lithological and chemical diversity of the samples. These authors interpreted the resulting age as due to a widespread metamorphic episode, at medium to high-grade level, which produced a pervasive Sr isotopic homogenisation affecting all lithological units, in the entire region. Only a few of the samples, and notably those collected in Paraguay, plotted clearly above the mentioned reference isochron. A few other, especially some of the felsic volcanic rocks, plotted below it, yielding younger calculated apparent ages.

The classification shown in table 2 into rock type and tectonic, for those samples collected by us (labelled RA), and available for study, was made based in the geological setting, as well as the petrographic and deformational features. The samples collected by the Radam survey in the 70's were classified by the lithology indicated in Araujo and others (1982), as well as by their location in the region. Many of the samples exhibit Rb content above 200 ppm and Sr content below 40 ppm. These samples with high Rb/Sr ratios are found in all the geological units, with the exception of the Rio Apa gneisses, but for this unit sampling is not sufficient. A granitic sample in Paraguay yielded the oldest value of 1835 Ma, while the youngest apparent age, of 1436 Ma, was obtained in a granophyre associated to the Alumiador intrusive body. Moreover, most of these apparent ages in high Rb/Sr samples fall within the 1600-1800 Ma interval. Very high $^{87}\text{Rb}/^{86}\text{Sr}$ values are always looked with suspicion, because of the different behaviour of Rb and Sr in the geochemical processes, and their different element mobility. However, the bulk of the collection already indicates the geochemical character of the entire region, where felsic magmatic rocks, usually rich in potassium, are predominant. Lacerda Filho and others (2004) considered as related to magmatic arcs both their Rio Apa and Amoguijá tectonic units. The former includes our Caracol leucocratic gneisses, and the latter includes the Alumiador granites and Serra da Bocaina volcanics.

Figures 6 A to D are Rb-Sr isochron-reference diagrams that were drawn taking into account reasonably coherent systems, possibly affected by the same episode of Sr homogenisation above mentioned, in which the analysed samples belong to the same tectonic unit, and were collected within reasonable distances from each other. They are related to the granitic rocks collected in Paraguay, the Caracol leucogneisses, the Alumiador granite, and the granitoid rocks near Baía das Garças, closely associated to the Alto Tererê metamorphics. It shall be bear in mind that such classification has unavoidable biases, because many of the samples have mixed character, especially those of the foliated felsic granitoid gneisses, which could belong to more than one category.

Figure 6 – Rb-Sr isochrones

Since only two samples from the Rio Apa gneisses were analysed, a Rb-Sr isochron diagram was not attempted. One sample of a banded gneiss near Morraria (4036 EG 28, location on fig. 5), and belonging to Rio Apa Complex, yielded a calculated age of 1648 ± 31 Ma (table 2). However, from the same area, two U-Pb zircon ages of about 1940 Ma were obtained (Appendix 2, figure 4A), related to the magmatic crystallization of the zircons.

The felsic volcanic rocks of the Serra da Bocaina Group, all dated by Araujo and others (1982), yielded varied and often much younger calculated apparent ages, between 1400 and 1700 Ma (table 2). Araujo and others (1982) attempted to calculate the age of a Rb-Sr errorchron for these samples, and reported an apparent age of 1650 Ma. In Appendix 2 a U-Pb SHRIMP zircon age of 1794 Ma is reported for a volcanic rock attributed to the Serra da Bocaina Group, collected near the Serra da Alegria.

The analytical points of five granitic samples collected in Paraguay and corresponding to granitoid rocks of the Paso Bravo Province of Wins (1986) plotted close to the best fit line of figure 6A, whose inclination would correspond to an age of 1846 ± 47 Ma, and a low $^{87}\text{Sr}/^{86}\text{Sr}$ initial ratio of 0.7028. Because of the very low Sr initial ratio, we suggest that such age value could be attributed to the magmatic formation of these granitic rocks. Sample RA 112, also from Paraguay, yielded a somewhat younger Rb-Sr calculated age, of about 1730 Ma (table 2). Regrettably, the attempted U-Pb zircon age determinations from that region (RA 95 and RA 111) were not successful, due to the high U content of the zircons, affected by strong Pb loss.

Seven samples of granitoid rocks, belonging to the Caracol leucogneisses, yielded a best fit line corresponding to a calculated age of 1674 ± 17 Ma (fig. 6B), with a $^{87}\text{Sr}/^{86}\text{Sr}$ initial ratio of 0.7098. This value is very likely related to the mentioned pervasive Sr isotopic homogenization episode, associated to the medium to high-grade metamorphic episode, responsible for the granoblastic texture shown by these rocks. From this unit, two U-Pb SHRIMP zircon ages are reported (RA 81 and RA 84), with Pb-Pb ages of 1720 and 1750 Ma. They are probably related to the igneous formation of the protoliths of these leucocratic gneisses, within a magmatic arc environment, and the Rb-Sr isochron age shall be related to the regional metamorphism that affected the tectonic unit.

Eight samples from the main outcrop of the Alumiador Granite plot close to the best fit line of figure 6C, corresponding to a calculated age of 1681 ± 47 Ma, and a $^{87}\text{Sr}/^{86}\text{Sr}$ initial ratio of 0.7057. This Rb-Sr age is comparable to the one obtained for the Caracol gneisses, but with a lower Sr initial ratio. In our interpretation, since the Alumiador granite was affected by a strong ductile deformation, such age is tentatively attributed to same pervasive regional deformational

episode. This Rb-Sr isochron age contrasts with the magmatic age of formation, detected by two good quality U-Pb ages around 1850 Ma (Appendix 2, fig. 4B). Two samples of potassic granites, and two granophyres, yielded much younger apparent ages, below 1500 Ma (table 2).

Several samples of granitoid rocks were collected in a small area, along the road MS 382, close to the locality of Baía das Garças (see fig. 3 and 5), not more than a few hundred meters from each other, and may be possibly considered cogenetic. They were analysed by the Rb-Sr and by the Sm-Nd methods to check their possible correlation with the Alumiador granite, but also to investigate the geologic history of the Alto Tererê metamorphics, to which they are associated. Twelve samples of granitoid rocks collected at Baía das Garças were analysed and their points were included in the diagram of figure 6D, together with three other samples collected from a similar granitic body located about 40 km to the north. The U-Pb zircon ages from two of these granitoid rocks (RA 35 and 40, see Appendix 2) yielded ages above 1740 Ma. The calculated best-fit line in the diagram of figure 6D corresponds to an age of 1635 ± 39 Ma, with a low $^{87}\text{Sr}/^{86}\text{Sr}$ initial ratio of 0.703. Three samples of the Baía das Garças area, all them with high Rb/Sr ratios, were excluded from the calculations of the best-fit line. One of them (RA 35A), yielded an apparent age of about 1600 Ma, when calculated with a $^{87}\text{Sr}/^{86}\text{Sr}$ initial ratio of 0.705, and two others (RA 36A and 36B) yielded apparent ages of slightly less than 1700 Ma (table 2).

In summary, the quite reasonable Rb-Sr reference isochrons obtained from three of the four groupings (Alumiador, Caracol and Baía das Garças) seem to be geologically significant, however, due to the high errors of the each calculation, the age values shall be taken with caution. It is difficult to consider that the calculated ages related to the best-fit lines would be different from each other. The three apparent ages, 1674 ± 17 Ma, 1681 ± 47 Ma and 1635 ± 39 Ma are well within the indicated errors, and perhaps only the 1635 Ma age could be seen as indicating a younger event. For the tectonic interpretations employed in this work, we will consider the existence of a strong regional metamorphism, at the medium to high level, responsible for a quite pervasive Sr isotopic homogenisation, with an age not far from 1680 Ma. The granitoid rocks from Paraguay were possibly formed at around 1850 Ma, and seem not having being affected by the strong Sr isotopic homogenisation reported for the other rocks.

Sm-Nd Determinations

Twenty eight Sm-Nd determinations are available for this work, 13 of which were published by Lacerda Filho and others, (2004). The location of the analysed samples, many of them also analysed by the Rb-Sr method, are displayed in figure 5. Analytical data are included in table 3, in which we kept the same classification used for table 2. The new set of samples was tentatively classified according to their position on the geological map.

Among the relevant analytical data, table 3 also brings the calculated Sm-Nd T_{DM} model ages and the $f_{\text{Sm}/\text{Nd}}$ values. In addition, it also presents the $\epsilon_{\text{Nd}(T)}$ values calculated for the estimated age of the immediate protolith of the rock unit, taken from the available U-Pb SHRIMP zircon determinations, as follows: 1940 Ma for the Rio Apa Complex; 1850 Ma for the Alumiador Suite and the Paso Bravo Province; 1790 Ma for the Serra da Bocaina volcanics and the Serra da Alegria magmatic suite, and 1750 Ma for the Caracol leucocratic gneisses and for the granitoid rocks near Baía das Garças.

The Sm-Nd T_{DM} model ages display three very coherent age groups:

1. The oldest one includes the Alumiador granites, the Serra da Alegria magmatic suite, and samples JV 1D and JV 15, located near the Serra da Alegria and attributed to the Rio Apa Complex. These samples yielded an average model age of 2.52 Ga.
2. A second group included the Caracol leucocratic gneisses, one sample of the Serra da Bocaina felsic volcanics and a few gneissic rocks attributed to the Rio Apa Complex, but associated in area with the Alto Tererê schists. Those samples yielded a mean model age of 2.23 Ga. Two granitoid rocks from Paraguay also showed Sm-Nd model ages close to this second group.
3. The youngest group includes most of the granitic rocks of the Baía das Garças, which yielded an average model age of 2.02 Ga. Two exceptions must be noted: sample RA 39, with a slightly older model age, and sample RA 36 B, which yielded the oldest Sm-Nd model age of the entire set, at 2.81 Ga. Moreover, sample RA 43, that was included within the Caracol gneisses in table 2, contrariwise showed complete affinity with the Baía das Garças granitoids, when the Sm-Nd analyses are considered.

Figure 7 is a Sm-Nd correlation diagram in which all analytical points are plotted. The samples are not cogenetic, therefore good quality and precise isochron lines shall not be expected. However, the diagram shows that the magmatic history of the rocks has produced significant fractionation between Sm and Nd, and a reasonable correlation enveloping all samples may be observed. Three coherent alignments are outlined by different colours in figure 7. Moreover, a strong correspondence is seen between each of them with one of the three groups of samples already envisaged from the direct analysis of table 3, enabling a tentative explanation in terms of age and geological evolution.

Figure 7 – Sm-Nd correlation diagram

In figure 7, samples JV-1D and JV-15, attributed to the Rio Apa gneisses from the northern part of the region, together with three samples of the Alumiador granitic suite, and a few samples from the Serra da Alegria magmatic suite (blue colour in fig. 7), plot close to a reference isochron with a late Archean age. In contrast, the samples of granitoid rocks occurring near Baía das Garças (red colour in fig. 7) are reasonably aligned along a much younger reference isochron, of Paleoproterozoic age. In between these two reference lines, two samples of the Caracol leucocratic gneisses, plus samples JV-18, JV-23, JV-24 and JV-30, attributed to the Rio Apa Complex, but occurring close to the region in which the Alto Tererê schists predominate (yellow colour in fig. 7), are aligned along an intermediate reference line. The close agreement of the groupings established with the Sm-Nd T_{DM} model ages of table 3, with those resulting in the Sm-Nd isochron diagram of figure 7, reinforce the inference that the Sm-Nd systems were not modified after their formation within the rock protoliths, and therefore the resulting age values have a geological significance.

The Nd isotopic signatures, shown in table 3, indicate that all the analysed samples, independently of their age or lithology, point to the operation of successive cycles of accretion tectonics, from the late Archean to the Lower Proterozoic. They also confirm the separation already envisaged in three groups when the Sm-Nd model ages are taken into account, as follows:

1. For the oldest group, which includes the Alumiador granites, the Serra da Alegria magmatic suite, and two of the Rio Apa gneisses (JV 1D and JV 15), the $\epsilon_{Nd(T)}$ is always

- negative, up to (-6), indicating a great deal of crustal reworking within the original magmatic chambers;
2. In contrast, for the youngest group, which comprises the granitoid rocks near Baía das Garças, the $\epsilon_{Nd(T)}$ are slightly positive, suggesting a predominant contribution of juvenile sources. Two exceptions are noted, RA 39 and RA 36B, which yielded negative $\epsilon_{Nd(T)}$ values. These samples are the same that were not aligned with the remaining granitoid rocks of Baía das Garças in figure 7.
 3. In the case of the second group, the $\epsilon_{Nd(T)}$ values discriminate two different sub-groups, suggesting different source material. The two analyzed samples of the Caracol leucocratic gneisses showed slightly negative values, around (-2). In contrast, the granitoid rocks attributed to the Rio Apa Complex, but associated to the Alto Tererê metamorphics (JV 18, JV 23, JV 24 and JV 30), yielded near zero or slightly positive values, when calculated for a tentative age of 1940 Ma, like in table 3. However, if an age of 1750 Ma is assumed, their $\epsilon_{Nd(T)}$ values are slightly negative, similar to those of the Caracol gneisses. Negative $\epsilon_{Nd(T)}$ values were also yielded by one sample of the Serra da Bocaina felsic volcanics, and by two samples of granitoid rocks of the Paso Bravo Province in Paraguay.

Figure 8 – Nd isotopic evolution diagram

Figure 8 is a Nd evolution diagram in which $\epsilon_{Nd(T)}$ values are plotted against the selected tentative ages attributed to the samples. At least four separated evolutionary patterns are indicated, suggesting derivation from different sources. One of them relates the Alumiador suite granites, that could be formed by reworking of ancient material similar to the Rio Apa Complex represented by samples JV 1D and JV 15. Another is related to the magmatic rocks of the Serra da Alegria suite, with their own evolutionary path. A third one seems to relate the granitoids of the Paso Bravo Province, the Caracol gneisses, the Serra da Bocaina volcanics, and the gneisses attributed to the Rio Apa, but associated to the Alto Tererê metamorphics. Finally, the Baía das Garças granitoids follow a quite different path, suggesting a major contribution of a juvenile source. As such, these rock units seem to have behaved as separated systems, making unsustainable the hypothesis of a derivation from each other.

K-Ar and $^{40}Ar/^{39}Ar$ Determinations

Seven K-Ar determinations and fifteen $^{40}Ar/^{39}Ar$ determinations are presently available from the studied area, and the location of the analyzed samples is shown in figure 9. The K-Ar analytical data are indicated in table 4. Three of them were obtained in biotite, in this work, and yielded quite concordant apparent ages around 1320 Ma. Four others were reported by Araujo and others (1982). One of these, from an amphibole with low K content, yielded a similar apparent age, close to 1370 Ma, but with a large experimental error. One muscovite and another amphibole, with higher K content, exhibited apparent ages close to 1270 Ma, and an third amphibole (578/EG 79) yielded a much lower apparent age of 850 Ma. Although these K-Ar results are not concordant, and are affected by large experimental errors, they already indicate the existence of a relevant Mesoproterozoic regional thermal event at about 1300 Ma.

Figure 9 – Location of samples dated by K-Ar and $^{40}Ar/^{39}Ar$ methods

This thermal episode is clearly confirmed by the fifteen $^{40}\text{Ar}/^{39}\text{Ar}$ determinations, obtained for different rocks within the entire region. The diagrams with the step-heating spectra are illustrated in figure 10. Table 5 brings a simplified list of the plateau and integrated ages, taken from the figures, but the complete analytical data are included in Appendix 3.

Figure 10 - $^{40}\text{Ar}/^{39}\text{Ar}$ step-heating spectra

Three biotite samples were run in triplicate, and five others in duplicate. With one exception, the results were very consistent. A few of the analyses showed some argon loss for the low temperature steps, but most of the analyses yielded good plateau ages. Only one of the analytical runs, for sample RA 62F, was unsuccessful. Five muscovite samples were also analyzed, all in duplicate, with good quality results. Two of the samples, RA 52 and RA 45, had most of the released gas in one step, but this seems not to have damaged the resulting age. However, in the case of the two amphiboles, the spectra are not of good quality. One of the runs for sample RA 88C was lost, and the resulting plateau depends on only two steps. For the second amphibole, RA 93A, the two analyses are not concordant, and both showed what appears to be excess argon 40.

The tight grouping of very precise plateau ages close to 1300 Ma is the most significant interpretative result, shown by seven biotites, five muscovites and amphibole RA 88C. In contrast, biotite RA 83 yielded a significant younger apparent age of about 1100 Ma.

As already indicated by Cordani and others (2005, 2008a, 2008b), the K-Ar and $^{40}\text{Ar}/^{39}\text{Ar}$ apparent ages close to 1300 Ma must be associated to a strong and widespread regional heating, with a temperature of at least 350 - 400 °C, necessary for the complete release of argon from all minerals, including a few amphiboles, that affected the entire region. In addition, younger and possibly localized thermal events are suggested by the ages obtained in samples 578/EG -79 (840 Ma) and RA 83 (1100 Ma), whose tectonic significance shall be investigated.

TECTONIC EVOLUTION

The already available radiometric data, discussed in the previous chapter, are very significant for the timing of relevant episodes within the Rio Apa Craton, and therefore for the interpretation of the regional tectonic evolution. In a general way, and taking into account all available data, most pre-Neoproterozoic basement rocks seem to be related to a series of magmatic arc complexes, whose material originated from different sources at different times. In effect, the Sm-Nd systematics (table 3, fig. 7 and 8) clearly point to variable proportions between juvenile and reworked component in the magmatic rocks, indicating divergent amounts of crustal components in the original magmas.

Figure 11 – Histogram of age determinations

Figure 11 is a general histogram in which all geochronological determinations (Sm-Nd T_{DM} model ages, Rb-Sr model ages of Rb-rich samples, K-Ar plus Ar-Ar ages) are taken into account. The unusual feature is that despite of the reasonably large number of determinations, there is no overlap among the ages obtained through the different dating methods. The Sm-Nd model ages are all older than 1.9 Ga, the Rb-Sr ages are all between 1.4 and 1.9 Ga, and the argon ages are

all younger than 1.4 Ga. The Sm-Nd T_{DM} model ages display three peaks, but only one is prominent for the Rb-Sr analyses, and another for the K-Ar and Ar-Ar analyses.

For the Sm-Nd method, the three peaks observed are related to the isotopic signature of the regional tectonic units, as a response to the nature of the original material and the particular characteristics of the crustal evolution. As shown in the pertinent item, the Alumiador granites and Serra da Alegria magmatic suite, and part of the gneisses considered Rio Apa, in the western part of the region, belong to the oldest group (about 2.5 Ga). The second group (2.3 Ga) comprises the Caracol gneisses, the Serra da Bocaina volcanics, and the Paso Bravo granitoid rocks. To the third group (2.0 Ga) belong the granitic rocks of Baía das Garças, associated to the Alto Tererê metamorphic rocks.

The position in time of the U-Pb SHRIMP zircon ages is also indicated in figure 11, related to the magmatic crystallization of the different units, all them formed during the Paleoproterozoic. The oldest age, 1940 Ma, was obtained from one granitoid gneiss of the Rio Apa magmatic arc of the northern part of the area. The second, 1850 Ma, marks the intrusion of the Alumiador suite. Finally, the youngest event, dated at about 1720 Ma is related to the establishment of the Caracol magmatic arc, more or less coeval to the granitic intrusions within the Alto Tererê schists at the Baía das Garças area. Two additional and relevant magmatic events, dated by only one sample each at about 1790 Ma, whose position was not indicated in figure 11, are the felsic volcanism of the Serra da Bocaina, and the gabbro-anorthositic magmatism of the Serra da Alegria suite.

For the Rb-Sr, K-Ar and Ar-Ar methods, they apply coherently in the entire region, independently of the character of the analysed samples. The tectonic interpretation of their results was already considered in the appropriate items, as follows:

1. A widespread regional Sr isotopic homogenization episode occurred at about 1680 Ma, connected to ductile tectonics in some rocks and a medium- to high grade pervasive metamorphism in others.
2. A regional heating affected the region at about 1300 Ma, attaining a temperature of at least 350-400 °C, as suggested by the argon blocking temperature in micas, also covering the whole of the area.

Taking into account the distribution of the Sm-Nd model ages, the region can be clearly separated into western and eastern domains, separated by a clear boundary, and therefore considered tentatively as two distinct tectonic blocks within the Rio Apa Craton. The western block would encompass the Rio Apa gneisses of the western basement, the Alumiador and the Serra da Alegria intrusions, the Amolar metasedimentary rocks, and the Serra da Bocaina felsic volcanics. The eastern block would include the Rio Apa gneisses of the Morraria area, the Alto Tererê schists, together with the Baía das Garças granitic rocks, the Caracol leucocratic gneisses, and the gneisses, granites and migmatites of the Paso Bravo Province.

Figure 12 – Tectonic units of the Rio Apa Craton

Figure 12 is a sketch map following such idea, placing the two tectonic blocks side by side, separated by a roughly meridian trending limit along the eastern border of the Alumiador granite. To the north, this tentative boundary will deflect to a NW-SE trend along the northern side of the Serra da Alegria. To the south, it will take a NE-SW trend along the Perdido river, and will deflect to a NNW-SSE trend in Paraguay, along the boundary of the Amolar metasediments. This inferred limit can be easily followed in the SLAR or in the satellite imageries, and Araujo and

others (1982) and by Godoy and others (1999) had already indicated some segments of it as large faults.

We speculate that this important discontinuity is a major transcurrent or transpressional fault zone, suturing two different tectonic domains that were juxtaposed at the time in which the principal regional deformation affected the entire area, at 1680 Ma, as suggested by the Rb-Sr systematics. The main compressional tectonic transport responsible for the welding of both terranes shall have been from East to West. Moreover, the eastern block, containing rock units formed at a lower crustal level than those of the western block, shall be the overriding terrane. From that time on, the unified Rio Apa block behave as one singular and tectonically stable cratonic mass.

Considering the available geological, petrological, geochemical, structural and geochronological data, as well the tectonic inferences, the geologic evolution of the Rio Apa cratonic fragment can be envisaged as follows:

1. A gneissic rock from the northern part of the region, near Morraria, yielded a Paleoproterozoic U-Pb zircon age of 1940 Ma, the oldest one in this part of the South American continent. The tectonic significance of it is still obscure, and tentatively it may be considered either as an outcrop of an exotic ancient terrain, or as a tectonic inlier within the younger Alto Tererê metamorphic rocks.
2. A small region of basement gneisses occurs at the western part of the region. Direct ages of these rocks are not available at present, and they are tentatively considered coeval to the similar rocks near Morraria of the northern region. They are intruded by the Alumiador Suite, from which two monzogranites yielded reliable U-Pb zircon ages of about 1850 Ma. Similar age is also encountered for some granitoids of the Paso Bravo Province in Paraguay, belonging to the eastern block and dated by the Rb-Sr method.
3. Near Porto Murtinho, overlying the western block, the felsic volcanics of the Serra da Bocaina Group outcrop, and a U-Pb zircon age of 1790 Ma was obtained by Lacerda Filho and others (2004). A similar age was also obtained from an anorthosite from the magmatic suite of the Serra da Alegria.
4. The Amolar metasedimentary rocks also belong to the western block. They are intruded by granitic rocks similar to the Alumiador suite, and therefore maybe older than 1850 Ma. However, other alternatives are possible for a younger age of the unit. For instance, (1) the intrusive granites may be much younger, and (2) they belong to a special structural setting such a mantled gneissic dome.
5. To the east-southeast of this area the Caracol orthogneisses occur, formed probably in a series of successive magmatic arcs between 1700 and 1760 Ma. These rocks may be coeval with gneissic rocks interbedded with the Alto Tererê schists, to the north, which are intruded by granitoids with similar ages, occurring near Baía das Garças. All these rocks, exhibiting granoblastic texture, were regionally metamorphosed at medium to high level at about 1680 Ma, as indicated by Rb-Sr work. The observed Sr isotopic homogenization at the whole-rock level enables us to estimate at more than 500°C the attained temperature for the metamorphism of the Caracol gneisses.
6. Near 1300 Ma ago, the Rio Apa craton was affected by a widespread regional heating, indicated by the several $^{40}\text{Ar}/^{39}\text{Ar}$ plateau ages on biotites and muscovites (fig. 10) when the temperature for the entire region probably surpassed 350°C. Unambiguous tectonic features related to this thermal episode have not yet been described. Perhaps one of them could be the shallow dipping foliation observed for the Caracol gneisses, at least along

the BR 267 profile, where neof ormation of micas was superimposed on the granoblastic texture.

7. At the eastern border of the Rio Apa Craton, the Paraguay-Araguaia belt was formed (Almeida, 1967), and its tectonic evolution occurred during the latest Neoproterozoic. Thrust faults related to the tectonic front of the Cuiabá Group are observed at the northeastern corner of figure 3 and figure 12, registering a tectonic transport from east-northeast. However, over the basement rocks, only a weak high-level brittle faulting is attributed to the Neoproterozoic tectonics.

8. The eastward low-angle dips of the Corumbá Group, and the western low-angle dips of the coeval Itapocumi Group (fig. 12) are likely to have been produced by high-level gentle folding, forming a structural high corresponding to the outcrops of the Rio Apa craton. Speculating again, this may be interpreted as a reflection of Andean mobility, related to plate convergence, and interaction of relatively small plates such Pampia or Arequipa-Antofalla (Ramos, 2008) possibly during the early Paleozoic. The moderate fold and thrust features at Valle-mi, suggested as part of an extensive folded belt by Campanha and Boggiani (2008) may be alternatively interpreted as an activated aulacogen, formed over the Rio Apa craton.

GEOTECTONIC CORRELATIONS

The Rio Apa cratonic fragment, whose regional tectonic evolution was described on the basis of geologic and geochronologic inferences, correlates well with the SW corner of the Amazonian Craton, where the granitic and gneissic Mesoproterozoic rocks of the Juruena-Rio Negro tectonic province (Tassinari and others, 1996), with ages between 1600 and 1780 Ma, are reworked by tectonic events related with the younger, adjacent, Rondonian-San Ignacio province (1560-1300 Ma, following Bettencourt and others, in press). A strong metamorphic imprint at about 1300 Ma is indicated by U-Pb ages on zircon rims and ^{40}Ar - ^{39}Ar dates on the country rocks (Santos and others, 2008; Cordani and Teixeira, 2007; Teixeira and others, 2006).

Almeida (1967) and later Alvarenga and others (2000) envisaged the Rio Apa craton as a direct prolongation of his named Guaporé Craton, which corresponds now to the southern half of the Amazonian Craton, because of the supposed continuity, along its eastern border, of the adjacent Neoproterozoic Paraguay folded belt. Nevertheless, large parts of the craton/ folded belt boundary are hidden below the recent sediments of the Pantanal basin, and the cratonic outcrops are not continuous. Because of this, a direct link between the Amazonian and the Rio Apa cratons is challenged, at least for the time before the Neoproterozoic.

Figures 1 and 2 indicate two possible alternatives, when the Rio Apa Craton is linked or not to the Amazonian Craton. The crucial feature is the Tucavaca belt, plotted in figure 2. Very likely it is a Neoproterozoic aulacogen, therefore an extensional structure, formed over continental crust. Considering the question in a larger scale, its tectonic determinant could be envisaged as a reflection of the crustal shortening episodes linked to the Paraguay belt, or alternatively a reflection of the contemporary extensional tectonic episodes, resulting from the separation of Laurentia and Amazonia. There may have been some tectonic dislocation between the two blocks along the Tucavaca belt. However, even if it was important, at least during the Neoproterozoic, the structural evidence points to a direct continuation of the Rio Apa cratonic fragment, as a prolongation of the Amazonian Craton.

For pre-Neoproterozoic times, the situation could be quite different, and will depend on the very complex interaction between Laurentia and Amazonia during the entire Proterozoic. These continental masses are considered to merge along a Grenville-Sunsás collisional belt at the end

of the Mesoproterozoic, around 1000 Ma. However, their interplay may have started much before, because plate convergence is observed in both cratonic nuclei, marked by successive and more or less synchronous accretionary and/or collisional episodes since the Paleoproterozoic.

In the Appalachian margin of Laurentia, the Labradorian, Pinwarian, Elsonian, Elzevirian, Shavinigan, Ottawan and Rigolet orogenic pulses are witnesses of the continued convergent efforts, lasting almost 1000 Ma, whose tectonic polarity was always directed to the West, towards the stable ancient craton (Gower and Krogh, 2002; Tollo and others, 2004; Bartholomew and others, in press). Only the last three tectonic pulses, Shavinigan, Ottawan and Rigolet, are considered to belong to the “Grenville orogeny”. On the other hand, in the southwestern margin of Amazonia, and during the same time-span, the Ventuari-Tapajós, the Rio Negro-Juruena, the Rondonian-San Ignacio and the Sunsás provinces were formed by successive partly accretionary and partly collisional pulses, always from NE to SW, keeping a tectonic polarity directed to the ancient core located to the North and Northeast (Cordani and Teixeira, 2007; Teixeira and others, in press).

Sadowski and Bettencourt (1996), in their article dealing with the Laurentia-Amazonia collision, envisage two complete Wilson cycles, with formation and disappearing of oceanic domains, and culminating with the Sunsás orogeny at the latest Mesoproterozoic, around 1000-1100 Ma, when Rodinia was forming. Moreover, as a precursor of the Sunsás orogeny, the Rondonian-San Ignacio orogeny is another major crustal event, active roughly between 1560 and 1300 Ma, affecting a large area along the Brazilian-Bolivian border (Bettencourt and others, in press). At least in part, it is synchronous with the Pinwarian and Elzevirian orogenies in Canada. In synthesis, Laurentia and Amazonia, after a complex and long lasting interplay, became welded at the end of Mesoproterozoic as part of Rodinia, and remained together until their separation at about 570 Ma, when the Iapetus Ocean was formed.

The repeated cycles of convergence-separation between Laurentia and Amazonia in the Mesoproterozoic produced a complex arrangement of allochthonous blocks with different size, trapped during the collisions of the main continental masses (fig. 13). They may have originated as disrupted parts of either Laurentia or Amazonia, or accretionary terranes newly formed within an intervening ocean (Ramos, 1988, 2009). One of the largest was the Paraguá block, partly accretionary and partly reworked crustal fragment, which was welded to the Rio Negro-Juruena province during the final tectonic events that characterize the Rondonian-San Ignacio orogeny. Later, it behaved as a stable cratonic landmass for the Sunsás belt (Litherland and others, 1989; Boger and others, 2005; Teixeira and others, in press). Relicts of other terranes, largely covered by Meso-Cenozoic sedimentary basins or by the Andean volcanic and sedimentary rocks, whose outcrops are dispersed over large distances, making correlations difficult, are the Arequipa, Antofalla, Pampia, among others (Ramos, 2008, 2009), and the Rio Apa block.

Figure 13 – Geotectonic sketch map of South America near the Precambrian-Cambrian boundary

The Arequipa and Antofalla terranes are key features for the Laurentia-Amazonia ties. They may have been produced during the separation of Laurentia from Gondwana at about 570 Ma (Li and others, 2008; Cordani and others, 2008), and could have returned later to South America, as allochthonous units, during the early Paleozoic. From their rocks, Paleoproterozoic to Paleozoic ages are available, indicating a very complex history (Ramos, 2008, 2009). Pampia is more enigmatic, since it is almost entirely overlain by the Phanerozoic sediments of the Chaco Basin.

The early Paleozoic sediments of the Puncoviscana Formation in northern Argentina (indicated in fig. 13) contain detrital zircons with Grenville-type ages, most probably from sources derived from Pampia (Zimmerman, 2005; Ramos, 2009). In contrast, older zircon crystals are very rare, indicating that such terrane, most likely, may be made up by accretionary systems of Grenvillian-Sunsás age, formed in the agglutination of Rodinia.

Possible correlations of the Rio Apa Craton with these allochthonous terranes, and with Amazonia, shall take into account the complex tectonic evolution of the former, where basement rocks of Paleoproterozoic age are affected by strong heating in the Mesoproterozoic. In this respect, the best possible correlation is with the SW portion of the Amazonian Craton, as indicated above, with the rocks of the Rio Negro-Juruena tectonic province. However, an alternative correlation can be made with the Paraguá block, where the main tectonic pattern was acquired during the Rondonian-San Ignacio orogeny, but where important Paleoproterozoic basement inliers are identified. These are the Lomas-Manechi medium-high-grade gneisses, described by Litherland and others (1989), and recently dated by U-Pb SHRIMP in zircon (Boger and others, 2005; Santos and others, 2008), yielding U-Pb zircon ages of 1660-1700 Ma, but also 1820 Ma. A correlation of the Rio Apa Craton with the Arequipa block can also be attempted, due to the older rocks of the latter (Loewy and others, 2004; Ramos, 2008). However, a correlation with either Antofalla or Pampia is more difficult, because these terranes seem to be made essentially by younger rocks, linked to the Sunsás orogeny.

A different kind of correlation can be made when one notices that large regions over Amazonia are affected by widespread heating at about 1200-1300 Ma, especially in its northern part. This Mesoproterozoic event, related to intra-plate heating in several large areas, accompanied by isotopic rejuvenation of micas, was named K'Mudku tectono-thermal episode by Barron (1969) in Guyana, and Nickerie metamorphic episode in Suriname and Colombia (Priem and others, 1971). This matter was thoroughly reviewed by Cordani and others (in press) for the entire Amazonian Craton, but the geodynamic significance of the pervasive heating remains a case of debate. However, as pointed out by Cordani and others (in press), extended areas affected by the K'Mudku/Nickerie event are located at the western limit of the Guiana Shield, adjacent to the Llanos Basin, foreland for the Andean mountain belt. Priem and others (1982), in eastern Colombia, obtained a few U-Pb zircon ages between 1560 and 1780 Ma, which allow to correlating them to the Rio Negro-Juruena province.

In figure 13, a tentative continuation of the Rondonian-San Ignacio province under the Solimões and Acre sedimentary basins is traced. In this case, the correlation with the Rio Apa Craton is likewise, because of the similar K-Ar and $^{40}\text{Ar}/^{39}\text{Ar}$ radiometric ages around 1300 Ma were obtained on separated minerals from older "basement" rocks. The physical significance of such apparent ages is the time of cooling below a critical temperature (about 350-400 °C), and may be interpreted in two ways, either as a response to some localized thermal event, or to the normal cooling associated to the regional uplift after cratonization of a certain area. For both Rio Apa and Paraguá tectonic blocks, the 1300 Ma apparent ages of micas shall be considered as related to crustal exhumation and cratonization of the Rondonian-San Ignacio orogeny. Following Cordani and others (in press), we assume that the similar regional cooling ages obtained in eastern Colombia by Priem and others (1971) indicate the extension of the Rondonian-San Ignacio Province, making up large parts of the Llanos Basin of Colombia and Venezuela (fig. 13).

In Bolivia, the Sunsás collisional belt is outcropping at the south-westernmost extremity of the Amazonian Craton, disposed parallel to and overprinting the Rondonian-San Ignacio

province. Figure 13 shows its possible continuation towards north-west, below the Phanerozoic basins, and bending further to the north, as proposed initially by Kroonenberg (1982), and more recently by many others, among which Ramos (2008 and 2009) and Cordani and others (in press). Good evidence for this is the Grenvillian/Sunsás-type age of detrital zircons in many Paleozoic sedimentary units, such as the already mentioned Puncoviscana Formation in Argentina, and the Paleozoic units adjacent to the Marañon massif in Peru, indicated in figure 13 (Cardona and others, 2009). Moreover, the Garzón Massif in Colombia, also indicated in figure 13, yielded K-Ar ages near 1000-1100 Ma (Jimenez and others, 2006), demonstrating that it was not affected by the Andean tectono-thermal episodes. We understand that the Marañon and Garzón massifs are the best evidence for the position of the western limits of the autochthonous or para-autochthonous basement to the Andean belt (fig. 13).

Figure 13 includes the proposed outline of the main geotectonic units discussed in the text, as suggested by the present authors at the time of agglutination of West Gondwana. The tentative outline of the Amazonian Craton, is given, and specifically its Mesoproterozoic tectonic provinces, considering the Paraguá block as the main constituent of the Rondonian-San Ignacio Province. As discussed above, the western and northern continuations of this province are outlined, as well those of the adjacent Sunsás Province. The allochthonous terranes of Paracas, Tahuín, Arequipa, Antofalla and Pampia, that were welded to Amazonia in Precambrian times, are also indicated in figure 13. Pampia has a special geotectonic significance, because it seems to be a direct continuation of the Sunsás mainly collisional belt. Since the detrital zircons received from Pampia show mainly magmatic arc derivation, it is possible that this terrane is made up by Grenvillian-type age accretionary material. Also the early Paleozoic Famatina belt, at the western margin of Pampia, includes detrital zircons with Grenvillian-type ages. Moreover, younger allochthonous terranes that were incorporated to South America during the Phanerozoic were shown in figure 13 (Ramos, 2009). Many of them include either basement inliers with Grenvillian-type ages, like the Chibcha and Tahami terranes of Colombia (Cordani and others, 2005b), or sedimentary rocks with detrital zircon, like the Cuyania or Chilenia terranes (Ramos, 2009). Finally, terranes agglutinated later, such as Patagonia, and the Meso-Cenozoic oceanic terranes of NW South America (Ramos, 2009) are also indicated in figure 13.

The Transbrasiliano lineament, cutting the continent from NE to SW, is the most relevant tectonic feature of South America in the Neoproterozoic, as the major suture along which a large ocean disappeared (Pimentel and others, 1997), in the process of agglutination of Gondwana. It includes the major Neoproterozoic intra-oceanic Goiás magmatic arc, witness of a large ocean separating a large supercontinent including Laurentia, Amazonia, Baltica and West Africa, from the large continental mass of São Francisco-Congo, plus smaller cratonic fragments, such as the Rio de La Plata, Luiz Alves and Paranapanema. The existence of such possibly very large oceanic domain made Kroner and Cordani (2003) and Cordani and others (2003) to suggest that the cratonic fragments occurring to the SE of the lineament may never had been parts of Rodinia. All Precambrian crustal nuclei plotted in figure 13 at the north-western side of the Transbrasiliano lineament show affinities with the Amazonian Craton, in which the Mesoproterozoic tectonic units of the Rondonian-San Ignacio and Sunsás belts are attached. In this way, rocks formed between roughly 1500 and 1000 Ma are predominant in the SW corner of Amazonia, and are also very common in the basement of the Andean belt. In contrast, the cratonic nuclei occurring at the south-eastern side of the Transbrasiliano lineament show affinities with the São Francisco-Congo Craton. The smaller cratonic nuclei, such as the Rio de La Plata, Paranapanema and Luiz Alves, large parts of which are hidden below the sediments of

the Paraná Basin, usually does not contain Mesoproterozoic domains, and were not affected by tectonic events of that age.

Therefore, both sides of the Transbrasiliano lineament show marked differences in their tectonic evolution. In the case of the Rio Apa cratonic fragment, its tectonic evolution bears a strong correlation with the north-western tectonic units, in which Mesoproterozoic elements are common. To the contrary, it shows no affinity at all with the south-eastern tectonic units.

ACKNOWLEDGEMENTS

This research received support from the Brazilian National Research Council (CNPq) through grants 302851/2004 to UGC and grants 471585/2007 and 308707/2006 to WT. Fruitful discussions with Fernando Wiens and Joffre Lacerda Filho are acknowledged. In addition, the authors received useful comments from several colleagues at USP, and especially B. B. Brito Neves, Jorge S. Bettencourt and Ginaldo Campanha. UGC is most grateful to Paulo Cesar Boggiani and Narciso Cubas, who accompanied him during field work in 2003.

APPENDIX 1

Analytical Methods

K-Ar and Ar-Ar methods

Table 4 reports seven geologically significant K-Ar determinations made in the regional rocks, and the location of the dated samples is shown in figure 9. All the analyses were obtained at the Geochronological Research Center of the University of São Paulo (CPGeo-USP), four of them at the time of the Radam Project (Araujo and others, 1982), and three other for the present work. The analytical procedures are described in Amaral and others (1996). Two aliquots from the same sample were separated for the K and Ar analysis. Potassium analyses of each pulverized sample were carried out in duplicate, by flame photometry. Argon extractions were made in an ultra-high-vacuum system, where a spike of ^{38}Ar was added and the gas was purified in titanium and copper getters. Final argon determinations were carried out in a Reynolds-type gas spectrometer. Analytical precision for K, based on the duplicate analyses, is usually below 4%, whereas for Ar it is around 0.5%. Decay constants for calculation are after Steiger and Jager (1977).

Fifteen mineral samples were dated by the ^{40}Ar - ^{39}Ar method, also at the CPGeo-USP, and the analytical procedures are described by Vasconcelos and others (2002). One of them has only one analysis, eleven were analysed in duplicate, and three of them in triplicate. Figure 10 shows the step-heating spectra, and table 5 reports a simplified list of the ^{40}Ar - ^{39}Ar ages. The complete analytical data are found in the Appendix III.

Rb-Sr method

Fifty Rb-Sr determinations, all them on whole-rock samples, were made at the CPGeo-USP on samples from the Rio Apa Craton. Half of them were already reported by Araujo and others (1982), and were re-discussed in this work together with the new Rb-Sr results. The location of the analysed samples is shown in figure 5. Analytical procedures were the same for the two sets of analyses, and are described in Tassinari and others (1996). Rb and Sr values were obtained by either X-ray fluorescence, or by isotope dilution, when Rb or Sr were below some critical value. $^{87}\text{Sr}/^{86}\text{Sr}$ ratios were measured with a Finnegan TH5 (the first set) or a Micromass VG-sector (the more recent set) mass spectrometers, and the isotopic ratios were corrected for isotopic fractionation during thermal ionization with $^{87}\text{Sr}/^{86}\text{Sr} = 0.1194$. Normal precision of the analyses is better than 2% for the Rb/Sr ratio, and better than 0.01% for the $^{87}\text{Sr}/^{86}\text{Sr}$ ratio. The analytical results are presented in Table 2.

Sm-Nd method

Cordani and others (2005) reported the first six Sm-Nd whole-rock determinations from the Rio Apa Craton, made by the CPGeo-USP. Nine others were obtained later in the same laboratory, for this work, from the granitoid rocks near Baía das Garças, and thirteen additional analyses were published by Lacerda Filho and others (2004), most of them from the northern part of the area. The location of the analysed samples was included in figure 5, and the analytical data are presented in Table 3.

The analytical procedures at the CPGeo-USP followed Sato and others (1995). The $^{143}\text{Nd}/^{144}\text{Nd}$ isotopic ratios were obtained in a multi-collector mass spectrometer Finnegan Mat, with analytical precision of 0.0014% (2σ). Experimental error for the $^{147}\text{Sm}/^{144}\text{Nd}$ ratios is of the order of 0.1%. La Jolla and BCR-1 standards yielded $^{143}\text{Nd}/^{144}\text{Nd} = 0.511849 \pm 0.000025$ (1σ) and 0.512662 ± 0.000027 (1σ) respectively during the period in which the analyses were performed. ϵ_{Nd} were calculated following De Paolo (1981), and the constants used include $^{143}\text{Nd}/^{144}\text{Nd}$ (CHUR) = 0.512638 and $^{147}\text{Sm}/^{144}\text{Nd}$ (CHUR)₀ = 0.1967. Lacerda Filho and others (2004) obtained their Sm-Nd determinations at the University of Brasilia. These analytical data are not available, but it is expected that they have an overall similar precision.

U-Pb SHRIMP method

U-Pb dating was carried out on single zircon crystals from eight samples, employing the SHRIMP II instrument of the Chinese Academy of Geological Sciences, operated from São Paulo using the SHRIMP Remote Operational System (SROS) device. Details of the analytical procedures are presented by Williams (1998). Correction for common Pb was made based on the measured ^{204}Pb , and the typical error component for the $^{206}\text{Pb}/^{238}\text{U}$ ratios is less than 2%. Uranium abundance and U/Pb ratios were calibrated against the TEM standard. The analytical results are displayed in Appendix II, and the apparent ages are shown in the Concordia diagrams of figures 2A to 2H. Four other measurements by the same method, reported by Lacerda Filho and others (2004), are also discussed in this work. They were obtained in Canberra, and presumably the same analytical procedures, following Williams (1998), were employed. However, the analytical data and the Concordia diagrams are not available. Three other U-Pb zircon determinations were made in other rocks of the region and their results were included, without specific comments, in Lacerda Filho and others (2004). The obtained apparent ages were considered of difficult interpretation (J. Lacerda Filho, written communication), and were not taken into account in this work.

APPENDIX 2
SHRIMP U-Pb data

Sample	% ²⁰⁶ Pb _c	U (ppm)	Th (ppm)	²³² Th/ ²³⁸ U (ppm)	²⁰⁶ Pb _{Rad} (ppm)	204corr ²⁰⁶ Pb/ ²³⁸ U Age (Ma)	1σ error	204corr ²⁰⁷ Pb/ ²⁰⁶ Pb Age (Ma)	1σ error	% Disc	²⁰⁷ Pb/ ²⁰⁶ Pb	% err	²⁰⁷ Pb/ ²³⁵ U	% err	²⁰⁶ Pb/ ²³⁸ U	% err
RIO APA (NORTH)																
RA-23.1	0.42	248	214	0.89	76.2	1962.5	25.0	1936	22	-1	0.1186	1.2	5.82	1.9	0.3559	1.5
RA-23.3	0.11	459	315	0.71	129.4	1828.8	22.6	1920	15	5	-	-	5.32	1.7	0.3280	1.4
RA-23.5	0.09	383	350	0.94	96.3	1654.3	20.5	1932	16	14	-	-	4.78	1.7	0.2926	1.4
RA-23.6	0.11	197	165	0.87	59.7	1949.7	25.9	1968	19	1	0.1208	1.1	5.88	1.9	0.3532	1.5
RA-23.9	0.00	228	148	0.67	68.0	1919.7	24.9	1955	17	2	0.1199	1.0	5.73	1.8	0.3469	1.5
RA-23.8	0.55	359	205	0.59	88.0	1609.9	20.3	1895	22	15	-	-	4.54	1.9	0.2837	1.4
PASO BRAVO PROVINCE																
RA-111-2.1	5.21	1845	645	0.36	270.7	967.1	22.7	1419	68	32	0.0897	3.6	2.00	4.4	0.1619	2.5
RA-111-3.1	1.04	1859	298	0.17	268.5	992.1	23.1	1525	22	35	0.0948	1.1	2.18	2.8	0.1664	2.5
RA-111-4.1	0.30	1492	253	0.18	286.0	1294.5	29.6	1544	16	16	-	-	2.94	2.7	0.2224	2.5
RA-111-5.1	0.94	905	235	0.27	173.5	1287.2	29.5	-	-	24	-	-	3.16	2.8	0.2210	2.5
RA-111-6.1	0.59	1222	337	0.29	211.1	1175.2	27.0	-	-	28	-	-	2.78	2.7	0.2000	2.5
RA-111-7.1	10.88	2378	1018	0.44	218.5	586.9	14.6	1491	127	61	-	-	1.22	7.2	0.0953	2.6
RA-111-8.1	1.72	2107	1009	0.50	233.4	769.3	18.2	1462	31	47	-	-	1.60	3.0	0.1268	2.5
RA-111-9.1	0.54	2760	1057	0.40	407.1	1016.5	23.5	-	-	20	-	-	1.96	2.6	0.1708	2.5
RA-111-10.1	4.37	1619	667	0.43	251.0	1026.6	24.0	1559	55	34	0.0966	2.9	2.30	3.9	0.1726	2.5
RA-111-11.1	7.14	1363	617	0.47	216.2	1020.3	24.7	1516	106	33	0.0944	5.6	2.23	6.2	0.1715	2.6
RA-95-1.1	3.20	2298	144	0.06	246.5	735.5	17.6	-	-	30	-	-	1.24	4.1	0.1209	2.5
RA-95-1.2	1.33	2269	231	0.11	251.7	773.1	18.6	1371	42	44	-	-	1.54	3.4	0.1274	2.6
RA-95-2.1	0.49	2337	1099	0.49	355.5	1046.3	24.3	-	-	31	-	-	2.29	2.6	0.1762	2.5
RA-95-3.1	6.37	2250	5227	2.40	149.3	449.9	11.3	1426	96	68	-	-	0.90	5.7	0.0723	2.6
RA-95-3.2	1.92	1209	1264	1.08	150.7	857.8	20.6	1535	48	44	-	-	1.87	3.6	0.1423	2.6
RA-95-4.1	4.52	1117	756	0.70	145.9	873.8	21.0	1410	73	38	-	-	1.79	4.6	0.1452	2.6
RA-95-5.1	1.61	311	128	0.42	51.4	1115.6	27.1	1397	61	20	0.0887	3.2	2.31	4.1	0.1889	2.6
RA-95-5.2	14.11	1427	1529	1.11	198.9	841.4	21.4	1472	177	43	-	-	1.77	9.7	0.1394	2.7

RA-95-6.1	1.85	219	17	0.08	38.3	1177.2	29.6	1323	102	11	0.0853	5.3	2.36	6.0	0.2004	2.8
RA-95-7.1	0.49	195	28	0.15	32.5	1137.9	29.4	1418	50	20	0.0897	2.6	2.39	3.9	0.1931	2.8
RA-95-8.1	0.56	420	74	0.18	73.0	1182.5	28.2	1355	41	13	0.0867	2.1	2.41	3.4	0.2013	2.6
RA-95-8.3	6.81	1418	821	0.60	148.5	693.7	17.1	1204	118	42	-	-	1.26	6.5	0.1136	2.6
RA-95-9.1	0.17	2224	246	0.11	430.3	1307.3	29.8	-	-	21	-	-	3.14	2.6	0.2248	2.5

ALUMIADOR GRANITIC SUITE

RA-77-1.1	0.23	190	147	0.80	52.2	1783.9	42.2	1879	27	5	0.1150	1.5	5.05	3.1	0.3188	2.7
RA-77-2.1	14.67	132	114	0.89	39.5	1673.3	48.1	-	-	8	0.1108	13.6	4.53	14.0	0.2964	3.3
RA-77-3.1	0.13	77	84	1.12	19.1	1626.3	43.2	1889	40	14	-	-	4.57	3.7	0.2870	3.0
RA-77-4.1	1.60	666	700	1.09	154.1	1515.9	34.9	1787	34	15	-	-	3.99	3.2	0.2651	2.6
RA-77-5.1	1.16	156	168	1.11	44.2	1816.4	45.4	1796	60	-1	0.1098	3.3	4.93	4.4	0.3255	2.9
RA-77-6.1	2.02	266	503	1.95	68.7	1664.6	39.0	1787	61	7	0.1093	3.4	4.44	4.3	0.2946	2.7
RA-77-7.1	0.15	773	680	0.91	207.2	1748.6	38.9	1820	13	4	0.1112	0.7	4.78	2.6	0.3116	2.5
RA-77-8.1	1.35	133	124	0.96	36.5	1763.7	43.5	1854	55	5	0.1134	3.0	4.92	4.1	0.3147	2.8
RA-77-9.1	5.28	98	82	0.87	15.2	1019.6	30.1	-	-	44	-	-	2.61	10.0	0.1714	3.2

CARACOL LEUCOCRATIC GNEISSES

RA-81-1.1	3.47	2071	2408	1.20	167.9	562.0	13.7	1378	57	59	0.0878	3.0	1.10	3.9	0.0911	2.5
RA-81-2.1	0.08	297	283	0.98	72.1	1600.9	36.7	1768	20	9	0.1081	1.1	4.20	2.8	0.2819	2.6
RA-81-2.1	0.40	503	1151	2.37	88.0	1190.7	27.8	1649	23	28	0.1013	1.3	2.83	2.9	0.2029	2.6
RA-81-5.1	0.46	523	616	1.22	63.3	846.3	20.4	1598	29	47	0.0986	1.5	1.91	3.0	0.1403	2.6
RA-81-6.1	0.15	664	206	0.32	50.7	548.1	13.5	539	44	-2	0.0582	2.0	0.71	3.2	0.0887	2.6
RA-81-7.1	1.24	887	1467	1.71	73.3	585.4	14.4	1512	41	61	0.0942	2.2	1.23	3.4	0.0951	2.6
RA-81-7.2	0.06	388	379	1.01	82.1	1419.8	32.9	1752	19	19	0.1072	1.1	3.64	2.8	0.2464	2.6
RA-81-8.1	3.99	679	1431	2.18	49.1	500.9	12.7	1450	93	65	0.0911	4.9	1.02	5.5	0.0808	2.6
RA-81-9.1	1.00	151	165	1.13	34.5	1508.0	37.7	1640	63	8	0.1008	3.4	3.66	4.4	0.2636	2.8
RA-81-10.1	0.79	824	1380	1.73	79.2	678.7	16.5	1451	34	53	0.0912	1.8	1.40	3.1	0.1110	2.6
RA-81-11.1	0.10	239	240	1.04	58.7	1620.0	44.5	1773	25	9	0.1084	1.4	4.27	3.4	0.2857	3.1

RA-84-1	0.20	121	85	0.72	31.9	1721.8	25.8	1724	29	0	0.1056	1.6	4.46	2.3	0.3062	1.7
RA-84-2	0.40	106	90	0.88	29.7	1811.0	27.8	1713	34	-6	0.1049	1.8	4.69	2.6	0.3244	1.8
RA-84-3	0.73	101	75	0.77	27.0	1741.2	27.3	1714	49	-2	0.1050	2.7	4.49	3.2	0.3101	1.8
RA-84-4	0.26	119	95	0.83	32.9	1794.1	26.9	1757	37	-2	0.1075	2.0	4.75	2.6	0.3209	1.7
RA-84-5	0.46	198	237	1.24	52.7	1734.4	23.0	1667	29	-4	0.1024	1.6	4.36	2.2	0.3087	1.5
RA-84-6	0.12	151	144	0.98	40.6	1751.1	24.8	1757	27	0	0.1075	1.5	4.63	2.2	0.3121	1.6

RA-84-6	0.87	92	71	0.80	24.8	1748.5	27.6	1709	58	-2	0.1047	3.1	4.50	3.6	0.3116	1.8
BAÍA DAS GARÇAS																
RA-35.1	0.32	254	257	1.05	64.7	1671.4	21.6	-	-	4	0.1067	1.4	4.35	2.1	0.2960	1.5
RA-35.2	2.38	446	345	0.80	82.7	1232.4	21.1	1499	150	18	0.0936	7.9	2.72	8.1	0.2107	1.9
RA-35.3.1	0.87	331	453	1.41	77.9	1548.9	19.9	1639	35	6	0.1008	1.9	3.78	2.4	0.2716	1.4
RA-35.3.2	0.54	263	282	1.11	62.6	1568.9	20.6	-	-	10	0.1067	1.6	4.05	2.2	0.2755	1.5
RA-35.5	0.50	553	264	0.49	102.9	1258.9	16.2	-	-	18	0.0951	1.4	2.83	2.0	0.2157	1.4
RA-35.6	16.61	2048	1197	0.60	140.8	416.5	6.9	1242	240	66	0.0818	12.3	0.75	12.4	0.0667	1.7
RA-35.7	3.55	357	584	1.69	58.4	1086.4	18.0	1662	72	35	0.1021	3.9	2.58	4.3	0.1836	1.8
RA-35.9	0.42	246	206	0.86	62.8	1672.9	22.3	1727	29	3	0.1057	1.6	4.32	2.2	0.2963	1.5
RA-40-2.1	0.96	319	229	0.74	54.7	1162.4	28.4	1710	43	32	0.1048	2.3	2.85	3.6	0.1976	2.7
RA-40-3.1	0.00	117	105	0.93	31.2	1739.6	43.9	1734	35	0	0.1062	1.9	4.53	3.4	0.3098	2.9
RA-40-4.1	0.24	210	109	0.54	54.4	1698.1	40.4	1765	30	4	0.1079	1.7	4.49	3.2	0.3014	2.7
RA-40-5.1	2.11	137	126	0.94	22.2	1089.9	28.8	1519	106	28	0.0946	5.6	2.40	6.3	0.1842	2.9
RA-40-6.1	2.15	302	238	0.82	73.7	1582.0	37.1	1796	50	12	0.1098	2.8	4.21	3.8	0.2781	2.6
RA-40-7.1	0.16	264	223	0.87	57.9	1464.2	34.8	1734	25	16	0.1062	1.4	3.73	3.0	0.2550	2.7
RA-40-8.1	2.00	254	141	0.57	37.9	1012.3	25.6	1734	74	42	0.1061	4.1	2.49	4.9	0.1700	2.7
RA-40-10.1	1.42	146	148	1.04	24.5	1134.0	29.5	1617	83	30	0.0996	4.5	2.64	5.3	0.1923	2.8

APPENDIX 3

Ar-Ar data

Sample	Material	Lab#	40/39	38/39	37/39	36/39	40*/39	%Rad	Ar40 (mols)	Laser (W)	Age (Ma)	± (Ma)		
SPA0301-93														
RAPA-88C	amphibole	1916-01A	371,35170	0,02280	5,19954	0,00912	370,33420	99,4	6,37E-14	0,30	1360,37	4,92		
		1916-01B	346,63370	0,02288	3,38744	0,00441	346,37230	99,7	7,03E-14	0,60	1297,47	5,66		
		1916-01C	337,23490	0,02535	10,05906	0,02138	333,92100	98,4	7,60E-15	0,90	1263,90	15,19		
		1916-01D	357,80760	0,13937	65,94290	0,17957	324,01170	86,6	1,44E-15	1,20	1236,73	107,34		
		1916-01E	335,90180	0,10489	58,14594	0,14864	308,36200	88,3	1,70E-15	3,18	1192,97	50,09		
RAPA-93A	amphibole	1917-01A	1542,3890	-0,00024	0,00000	0,11885	1507,2610	97,7	6,56E-15	0,30	3101,93	154,58		
		1917-01B	724,26660	0,01489	14,51466	0,02359	725,38710	99,2	4,38E-14	0,60	2101,09	11,99		
		1917-01C	398,80850	0,02295	57,00546	0,02389	411,69880	99,3	4,74E-15	0,89	1464,04	47,07		
		1917-01D	456,95850	0,05818	115,08640	0,10097	471,99520	95,4	1,60E-15	1,29	1605,22	68,92		
		1917-01E	419,98390	0,02865	52,27008	0,02828	430,57240	99,0	4,95E-15	3,17	1509,43	27,48		
		1917-02A	498,16960	0,01870	0,00000	0,03785	486,98340	97,8	1,87E-14	0,35	1638,67	18,00		
		1917-02B	523,40540	0,01305	15,55775	0,01558	525,41640	99,4	3,41E-14	0,50	1721,70	8,92		
		1917-02C	329,10280	0,02859	15,38201	0,02787	325,37260	97,9	7,40E-15	0,60	1240,48	15,20		
		1917-02D	376,87670	0,01146	0,92564	-0,00464	378,55120	100,4	6,58E-15	0,89	1381,44	25,92		
		1917-02E	356,41090	0,01800	18,68822	0,01989	356,39010	98,8	4,10E-15	1,39	1324,03	27,98		
		1917-02F	357,97810	0,01179	10,32250	0,01024	358,19680	99,4	1,26E-14	2,99	1328,78	12,91		
		RAPA-112	biotite	1918-01A	315,62010	0,01356	0,00259	0,00729	313,46590	99,3	9,83E-14	0,15	1207,36	4,18
				1918-01B	345,09810	0,01293	0,00000	0,00132	344,70880	99,9	1,29E-13	0,25	1293,02	3,30
				1918-01C	342,92520	0,01230	0,00000	0,00343	341,91140	99,7	5,87E-14	0,32	1285,51	10,01
				1918-01D	343,22770	0,01273	0,00000	0,00048	343,08630	100,0	5,73E-14	0,45	1288,67	5,29
1918-01E	338,87810			0,01575	0,05961	0,00602	337,11590	99,5	3,18E-14	0,55	1272,57	7,74		
1918-01F	352,02800			0,01231	0,00000	0,00023	351,95890	100,0	8,68E-15	0,65	1312,33	18,20		
1918-01G	351,33480			0,00503	0,00000	-0,01321	355,23840	101,1	6,47E-15	0,80	1321,00	18,51		
1918-01H	340,55870			0,01727	0,00000	0,00900	337,89990	99,2	1,07E-14	1,09	1274,69	14,85		
1918-01I	313,46890			0,01621	0,00000	0,03729	302,44800	96,5	4,32E-15	2,97	1176,15	22,98		
1918-02A	19,59212			2,14722	346,03190	2,66453	-960,8817	-	-2,66E-18	0,08	0,00	12718		
1918-02B	278,26120			0,01407	0,05565	0,00723	276,13780	99,2	5,75E-14	0,15	1099,37	4,22		
1918-02C	337,04310	0,01332	0,06920	0,00155	336,60500	99,9	8,81E-14	0,20	1271,19	3,78				
1918-02D	343,92190	0,01349	0,24157	0,00104	343,68760	99,9	5,93E-14	0,25	1290,28	4,40				
1918-02E	350,31260	0,01145	0,00000	-0,00021	350,37460	100,0	6,93E-14	0,35	1308,13	5,15				

		1918-02F	343,17650	0,01170	0,00000	0,00030	343,08820	100,0	5,56E-14	0,50	1288,68	5,81
		1918-02G	343,02480	0,00834	0,00000	-0,00448	344,34910	100,4	4,43E-14	0,70	1292,06	5,97
		1918-02H	336,23750	0,01189	1,27786	0,00194	336,04780	99,9	2,54E-14	3,19	1269,68	8,75
		1918-03A	253,19600	0,01120	0,00000	0,01272	249,43740	98,5	4,19E-15	0,08	1017,96	19,25
		1918-03B	326,07200	0,01584	0,31132	0,00792	323,82290	99,3	5,01E-14	0,15	1236,21	4,85
		1918-03C	345,07100	0,01258	0,00000	0,00147	344,63550	99,9	5,60E-14	0,20	1292,82	5,84
		1918-03D	346,27530	0,01054	0,00000	-0,00005	346,28800	100,0	3,54E-14	0,25	1297,24	16,05
		1918-03E	348,09590	0,01649	0,19247	0,00804	345,77880	99,3	4,87E-14	0,35	1295,88	6,15
		1918-03F	336,39820	0,01151	0,00000	0,00237	335,69830	99,8	4,03E-14	0,50	1268,73	6,56
		1918-03G	327,87980	0,02025	0,19317	0,00995	324,99590	99,1	2,36E-14	0,70	1239,45	9,88
		1918-03H	319,34160	0,02032	0,58256	0,01260	315,78600	98,8	1,55E-14	3,19	1213,86	12,08
RAPA-114	biotite	1919-01A	155,27340	0,03409	1,05401	0,05953	137,86120	88,7	4,98E-15	0,10	631,36	11,64
		1919-01B	335,77000	0,01487	0,00000	0,00365	334,68990	99,7	1,45E-13	0,20	1265,99	4,02
		1919-01C	346,82100	0,01466	0,00000	0,00213	346,19200	99,8	1,94E-13	0,30	1296,99	3,04
		1919-01D	353,09870	0,01477	0,03341	0,00260	352,34050	99,8	2,34E-13	0,45	1313,34	3,04
		1919-01E	348,82440	0,01379	0,00342	0,00139	348,41490	99,9	1,23E-13	0,55	1302,92	3,30
		1919-01F	350,99600	0,01441	0,03544	0,00199	350,41860	99,8	1,14E-13	0,70	1308,25	4,21
		1919-01G	349,10380	0,01378	0,00000	0,00090	348,83750	99,9	8,36E-14	0,90	1304,04	9,03
		1919-01H	349,37270	0,02191	0,75921	0,01062	346,46940	99,1	2,28E-14	1,39	1297,73	7,75
		1919-01I	350,39310	0,03611	0,00000	0,00950	347,58720	99,2	1,70E-15	2,34	1300,71	55,36
		1919-02A	258,70690	0,01060	0,04029	0,02634	250,93200	97,0	1,97E-14	0,12	1022,62	7,22
		1919-02B	339,12630	0,01498	0,01500	0,00284	338,29080	99,8	1,45E-13	0,20	1275,75	3,25
		1919-02C	349,82020	0,01114	0,00000	0,00026	349,74350	100,0	1,34E-13	0,25	1306,45	3,91
		1919-02D	346,97010	0,01433	0,00000	0,00193	346,39840	99,8	1,73E-13	0,35	1297,54	3,89
		1919-02E	348,61320	0,01569	0,03412	0,00488	347,18270	99,6	8,30E-14	0,40	1299,63	4,18
		1919-02F	347,36710	0,01518	0,00000	0,00147	346,93400	99,9	1,40E-13	0,50	1298,97	3,52
		1919-02G	344,85810	0,01355	0,00000	-0,00115	345,19800	100,1	1,57E-13	0,70	1294,33	3,67
		1919-02H	342,77540	0,01198	0,00000	-0,00050	342,92280	100,0	7,26E-14	0,90	1288,23	4,89
		1919-02I	340,30340	0,00212	0,01288	-0,00047	340,44420	100,0	1,40E-14	1,39	1281,56	15,61
		1919-02J	351,90630	0,00667	0,00000	-0,01212	355,48710	101,0	8,63E-15	3,19	1321,65	24,48
RAPA-114	biotite	1919-03A	-1,91902	0,49339	135,61400	0,55883	-171,9407	-	-2,92E-19	0,12	-1333,92	2201
		1919-03B	324,80350	0,01617	0,00000	0,01000	321,84900	99,1	2,10E-13	0,20	1230,74	4,37
		1919-03C	343,50210	0,01572	0,00000	0,00176	342,98150	99,8	1,19E-13	0,25	1288,39	4,61
		1919-03D	349,70230	0,01385	0,01654	0,00340	348,70160	99,7	2,55E-13	0,35	1303,68	3,33
		1919-03E	347,95210	0,01413	0,00000	0,00198	347,36670	99,8	2,06E-13	0,40	1300,12	4,60
		1919-03F	350,01980	0,01551	0,06576	0,00297	349,16250	99,8	1,65E-13	0,50	1304,91	3,83

		1919-03G	348,13230	0,01451	0,05530	0,00202	347,55350	99,8	2,31E-13	0,70	1300,62	4,85
		1919-03H	338,80170	0,01485	0,05196	0,00151	338,36990	99,9	9,37E-14	0,90	1275,97	4,08
		1919-03I	340,34590	0,01421	0,00270	0,00099	340,05270	99,9	1,65E-13	3,19	1280,51	3,38
RAPA-83	biotite	1920-01A	73,82641	0,00486	0,00000	0,00112	73,49490	99,6	4,48E-15	0,10	363,73	4,12
		1920-01B	258,48450	0,01087	0,00000	0,00105	258,17470	99,9	1,06E-13	0,20	1045,01	3,27
		1920-01C	287,32670	0,01202	0,00000	0,00045	287,19370	100,0	2,72E-13	0,30	1132,03	2,40
		1920-01D	288,60560	0,01220	0,01934	0,00072	288,39790	99,9	3,21E-13	0,45	1135,56	2,45
		1920-01E	285,54810	0,01067	0,00000	-0,00123	285,91190	100,1	1,12E-13	0,55	1128,28	3,79
		1920-01F	284,51540	0,01219	0,02585	-0,00044	284,65250	100,0	1,20E-13	0,80	1124,58	4,48
		1920-01G	263,08380	0,00915	0,00000	-0,00373	264,18390	100,4	1,89E-14	1,39	1063,38	7,14
		1920-01H	231,74210	0,01027	0,00000	-0,00126	232,11450	100,2	2,74E-14	2,55	963,11	5,53
		1920-02A	191,84380	0,04560	0,00000	0,14533	148,89970	77,6	2,48E-14	0,12	673,52	5,34
		1920-02B	262,55290	0,01692	0,00000	0,03049	253,54310	96,6	1,46E-13	0,22	1030,72	4,23
		1920-02C	269,55410	0,01357	0,00000	0,01042	266,47530	98,9	1,20E-13	0,30	1070,33	3,37
		1920-02D	270,54530	0,01282	0,06926	0,00801	268,19570	99,1	6,54E-14	0,35	1075,54	7,91
		1920-02E	272,76560	0,01848	0,02007	0,00663	270,81170	99,3	4,87E-14	0,40	1083,42	4,80
		1920-02F	272,82620	0,01587	0,20380	0,00445	271,56330	99,5	3,82E-14	0,45	1085,68	5,20
		1920-02G	271,26550	0,01540	0,00000	0,00512	269,75200	99,4	3,43E-14	0,55	1080,23	4,40
		1920-02H	273,62810	0,01273	0,08968	0,00560	271,99710	99,4	3,49E-14	0,80	1086,98	6,11
		1920-02I	265,16030	0,01799	0,00000	0,00947	262,36170	98,9	2,15E-14	1,49	1057,83	5,76
		1920-02J	288,61740	-0,01752	0,00000	-0,02691	296,56430	102,8	3,32E-15	3,18	1159,26	23,42
		1920-03A	236,55590	0,01043	0,00000	0,00536	234,97240	99,3	2,92E-14	0,12	972,27	4,89
		1920-03B	274,49300	0,01176	0,00000	0,00124	274,12690	99,9	1,53E-13	0,23	1093,37	2,97
		1920-03C	278,62680	0,01289	0,00000	0,00152	278,17730	99,8	9,15E-14	0,30	1105,44	3,41
		1920-03D	278,04190	0,01394	0,11892	0,00260	277,30330	99,7	7,63E-14	0,40	1102,84	4,52
		1920-03E	277,02710	0,01128	0,12382	-0,00004	277,07190	100,0	5,17E-14	0,50	1102,15	4,80
		1920-03F	273,74090	0,01103	0,20499	-0,00086	274,04690	100,1	3,55E-14	0,60	1093,13	6,42
		1920-03G	273,70690	0,01305	0,12665	-0,00092	274,01260	100,1	2,90E-14	0,80	1093,02	6,52
		1920-03H	272,87950	0,00753	0,00000	-0,00461	274,23960	100,5	2,76E-14	1,59	1093,70	5,68
		1920-03I	242,07820	0,09743	9,19147	0,06888	223,80780	91,9	1,43E-15	3,19	936,20	42,01
RAPA-76	biotite	1921-01A	330,10000	0,01282	0,00000	0,00489	328,65440	99,6	1,58E-13	0,20	1249,51	2,83
		1921-01B	350,38150	0,01200	0,11852	0,00055	350,25470	100,0	2,95E-13	0,35	1307,81	2,75
		1921-01C	348,12070	0,01178	0,00000	0,00082	347,87840	99,9	2,31E-13	0,50	1301,49	2,80
		1921-01D	346,13250	0,01081	0,06724	0,00048	346,01040	100,0	1,68E-13	0,80	1296,50	3,51
		1921-01E	341,45200	0,01137	2,52722	0,00358	341,16010	99,7	3,22E-14	3,17	1283,49	8,65

		1921-02A	343,53270	0,01235	0,50958	0,00349	342,65610	99,7	1,22E-13	0,20	1287,52	3,77
		1921-02B	349,18900	0,01259	1,07929	0,00192	348,95500	99,9	8,94E-14	0,30	1304,36	4,01
		1921-02C	347,16060	0,01406	1,08806	0,00210	346,87490	99,8	7,85E-14	0,50	1298,81	4,54
		1921-02D	347,67010	0,02051	2,82736	0,00500	347,06090	99,6	2,11E-14	2,99	1299,31	8,58
		RAPA-52 muscovite										
		1922-01A	144,73340	0,33390	8,20823	0,08414	121,22350	83,3	3,13E-16	0,20	565,90	85,59
		1922-01B	382,34880	-0,03042	0,00000	-0,06373	401,17420	104,9	1,48E-15	0,35	1438,22	68,93
		1922-01C	368,14540	0,05962	0,00000	0,04712	354,23010	96,2	4,15E-15	0,50	1318,34	32,98
		1922-01D	346,07070	0,01240	0,55336	0,00229	345,56330	99,8	2,55E-13	0,89	1295,31	2,87
		1922-01E	328,06950	0,03132	17,44110	-0,01132	336,65650	101,4	5,22E-15	3,18	1271,33	30,90
		1922-02A	344,27200	0,01399	0,00000	0,00302	343,37950	99,7	1,43E-13	0,50	1289,46	5,34
		1922-02B	344,01200	0,01656	1,63503	0,00309	343,59620	99,8	2,81E-14	0,65	1290,04	7,31
		1922-02C	349,41650	0,01914	0,00000	-0,03659	360,23030	103,1	4,67E-15	0,85	1334,11	25,70
		1922-02D	337,67460	0,01811	0,00000	-0,00278	338,49720	100,2	2,05E-14	2,99	1276,31	7,96
		RAPA-62F biotite										
		1923-01A	264,01940	0,01631	0,27636	0,01683	259,11360	98,1	9,02E-14	0,20	1047,89	3,23
		1923-01B	302,80500	0,01492	0,00000	0,01181	299,31480	98,8	7,58E-14	0,35	1167,18	3,18
		1923-01C	301,50270	0,01557	0,00000	0,00664	299,54190	99,3	3,42E-14	0,50	1167,83	5,70
		1923-01D	308,55080	0,01590	0,33412	0,00650	306,72380	99,4	2,60E-14	0,80	1188,32	6,62
		1923-01E	312,97060	0,00946	2,93372	0,00100	313,51100	100,0	1,47E-14	3,17	1207,48	14,04
		RAPA-62F biotite										
		1923-02A	315,64240	0,01277	0,26114	0,00437	314,42550	99,6	6,22E-14	0,15	1210,05	3,60
		1923-02B	345,66550	0,01204	0,00205	0,00183	345,12580	99,8	1,70E-13	0,30	1294,14	2,89
		1923-02C	345,71940	0,01209	0,00000	0,00070	345,51270	99,9	9,37E-14	0,50	1295,17	3,35
		1923-02D	347,13210	0,00340	0,00000	-0,00377	348,24310	100,3	2,11E-14	3,19	1302,46	9,16
		SPA0301-94										
		RAPA-18B muscovite										
		1926-01A	115,12450	0,01716	0,00000	0,01014	112,12960	97,4	1,65E-14	0,20	509,81	3,15
		1926-01B	114,11300	0,01174	0,00000	0,00027	114,03330	99,9	1,57E-13	0,35	517,33	1,20
		1926-01C	114,27810	0,00961	0,00000	-0,00232	114,96150	100,6	4,71E-15	0,50	520,99	7,09
		1926-01D	115,61440	0,01636	0,00000	-0,00018	115,66940	100,0	1,00E-14	0,89	523,77	4,40
		1926-01E	110,45910	0,02055	1,04504	0,00746	108,41170	98,1	4,80E-15	3,18	495,02	5,82
		1926-02A	115,54940	0,01496	1,07384	0,00921	112,98970	97,7	1,81E-14	0,20	513,21	2,78
		1926-02B	114,70460	0,01199	0,01031	0,00051	114,55570	99,9	1,20E-13	0,27	519,39	1,34
		1926-02C	113,04610	0,01187	0,05705	0,00074	112,83430	99,8	1,01E-13	0,40	512,59	1,11
		1926-02D	112,87520	0,00677	0,00000	0,00061	112,69270	99,8	8,20E-15	0,90	512,03	4,28
		1926-02E	115,19670	0,01080	0,00000	0,00067	114,99830	99,8	2,08E-14	2,99	521,13	2,63

RAPA-22	muscovite	1927-01A	318,01740	0,02967	0,00000	0,02984	309,20070	97,2	5,26E-15	0,20	1158,42	21,49
		1927-01B	359,34840	0,01213	0,00000	-0,00013	359,38600	100,0	2,92E-13	0,35	1292,08	2,56
		1927-01C	355,39430	0,01129	0,07428	0,00028	355,33430	100,0	5,64E-13	0,55	1281,65	2,42
		1927-01D	356,17610	0,01055	0,00000	0,00092	355,90460	99,9	1,40E-13	0,90	1283,12	3,55
		1927-01E	354,34530	0,01201	0,41050	0,00118	354,12280	99,9	1,25E-13	3,18	1278,52	3,33
		1927-02A	354,42550	0,00989	0,00000	0,00121	354,06650	99,9	1,19E-13	0,25	1278,37	3,38
		1927-02B	356,97770	0,01260	0,33789	0,00036	356,97820	100,0	3,41E-13	0,35	1285,89	2,98
		1927-02C	349,68720	0,01317	0,00000	-0,00038	349,79830	100,0	1,10E-13	0,50	1267,30	11,80
		1927-02D	358,08950	0,01240	0,00000	0,00133	357,69540	99,9	5,83E-14	0,89	1287,73	5,23
		1927-02E	357,75250	0,01406	1,49076	0,00337	357,22460	99,8	3,23E-14	2,99	1286,52	6,76
RAPA-23	biotite	1929-01A	320,24010	0,01249	0,00000	0,00572	318,55010	99,5	1,03E-13	0,20	1184,08	3,00
		1929-01B	345,81330	0,01346	0,06703	0,00239	345,12580	99,8	1,66E-13	0,35	1255,09	3,22
		1929-01C	350,95530	0,01172	0,00000	-0,00016	351,00330	100,0	8,51E-14	0,50	1270,43	5,37
		1929-01D	351,59610	0,01017	0,00000	-0,00311	352,51500	100,3	3,50E-14	0,80	1274,35	6,48
		1929-01E	348,38590	0,00106	0,00000	-0,00451	349,71500	100,4	2,58E-14	3,18	1267,08	7,96
		1929-02A	324,91670	0,01377	0,00000	0,00348	323,88920	99,7	8,38E-14	0,15	1198,57	4,56
		1929-02B	342,32910	0,01259	0,00000	0,00005	342,31500	100,0	3,00E-13	0,25	1247,71	14,03
		1929-02C	354,57770	0,01143	0,00000	-0,00036	354,68490	100,0	2,01E-13	0,35	1279,97	4,58
		1929-02D	350,33550	0,01092	0,00000	0,00060	350,15740	99,9	2,45E-13	0,50	1268,23	3,27
		1929-02E	351,22620	0,01057	0,00000	0,00006	351,20770	100,0	2,42E-13	2,99	1270,96	2,60
RAPA-32	muscovite	1930-01A	362,13970	0,01157	0,00000	0,00127	361,76330	99,9	2,26E-13	0,25	1298,17	2,63
		1930-01B	363,01700	0,01019	0,00000	-0,00131	363,40210	100,1	1,13E-13	0,40	1302,36	3,97
		1930-01C	368,26180	-0,00369	4,94649	0,01380	365,76060	99,0	1,12E-14	0,60	1308,37	18,59
		1930-01D	378,29170	-0,02844	0,00000	-0,05135	393,46040	104,0	7,03E-15	0,85	1377,50	22,91
		1930-01E	365,59070	0,00967	0,00000	0,00004	365,57820	100,0	4,87E-14	2,76	1307,91	6,42
		1930-02A	310,10350	0,00918	16,61129	0,03844	303,36270	96,8	4,62E-15	0,12	1142,20	26,68
		1930-02B	364,27660	0,01309	0,00000	0,00203	363,67500	99,8	1,41E-13	0,25	1303,06	3,17
		1930-02C	362,01640	0,01308	0,02186	0,00067	361,82500	99,9	3,20E-13	0,40	1298,33	2,57
		1930-02D	358,32400	0,01305	2,14223	0,00081	358,76020	100,0	7,08E-14	0,89	1290,47	4,90
		1930-02E	362,83440	0,01516	0,00000	0,00053	362,67900	100,0	3,34E-14	2,99	1300,51	8,56
RAPA-37A	biotite	1932-01A	347,03750	0,01396	0,74098	0,00128	346,88750	99,9	1,01E-13	0,15	1259,71	3,70
		1932-01B	365,24460	0,01047	0,00000	-0,00103	365,54930	100,1	1,38E-13	0,25	1307,83	2,81

		1932-01C	367,68970	0,01134	0,00000	-0,00015	367,73430	100,0	1,05E-13	0,35	1313,38	3,97
		1932-01D	360,87190	0,00790	0,77881	0,00198	360,53220	99,9	6,82E-14	0,55	1295,02	4,10
		1932-01E	351,25780	0,02503	6,84894	0,00907	350,69880	99,4	1,45E-14	2,76	1269,64	10,94
		1932-02A	326,76850	0,01503	0,99708	0,00584	325,33610	99,5	4,12E-14	0,15	1202,48	5,98
		1932-02B	360,35710	0,01367	0,57449	0,00192	359,97060	99,9	1,71E-13	0,25	1293,58	3,36
		1932-02C	365,11730	0,01235	0,00000	0,00051	364,96760	100,0	2,40E-13	0,35	1306,35	3,17
		1932-02D	366,54860	0,01278	0,00000	0,00057	366,38050	100,0	2,21E-13	0,50	1309,95	2,95
		1932-02E	367,98950	0,01163	0,00000	0,00033	367,89120	100,0	3,82E-13	2,99	1313,78	2,67
RAPA-33	muscovite	1933-01A	364,12390	0,01300	0,00000	0,00130	363,73820	99,9	1,25E-13	0,25	1303,22	4,05
		1933-01B	364,79110	0,01372	0,00000	0,00039	364,67470	100,0	7,59E-14	0,40	1305,61	4,70
		1933-01C	359,83540	0,01212	1,53405	-0,00104	360,62620	100,1	3,93E-14	0,60	1295,26	7,11
		1933-01D	359,55400	0,01811	3,20779	0,00529	359,00180	99,6	3,29E-14	0,80	1291,09	6,66
		1933-01E	360,38230	0,01531	0,46671	0,00143	360,10600	99,9	4,50E-14	2,34	1293,93	7,22
		1933-02A	320,76410	0,02415	0,00000	0,00901	318,10270	99,2	1,75E-15	0,15	1182,86	59,54
		1933-02B	363,19170	0,01336	0,00000	0,00507	361,69440	99,6	1,05E-13	0,35	1298,00	3,88
		1933-02C	361,68560	0,01509	0,01705	0,00603	359,90760	99,5	4,61E-14	0,80	1293,42	7,07
		1933-02D	364,02710	0,01166	0,00000	-0,00114	364,36450	100,1	3,76E-14	2,99	1304,81	6,96
RAPA-38	biotite	1935-01A	359,28860	0,01007	0,00000	-0,00177	359,81010	100,1	1,13E-13	0,15	1293,17	3,63
		1935-01B	366,37180	0,01091	0,00000	0,00045	366,23800	100,0	1,04E-13	0,25	1309,58	3,90
		1935-01C	361,60640	0,00794	0,00000	-0,00148	362,04310	100,1	6,97E-14	0,35	1298,89	6,03
		1935-01D	367,66780	0,00203	0,00000	-0,00452	369,00240	100,4	2,68E-14	0,55	1316,60	10,55
		1935-01E	380,36190	0,02045	0,00000	0,00483	378,93640	99,6	8,45E-15	2,34	1341,58	23,19
		1935-02A	10,64113	1,76425	871,05140	2,15591	-1319,760	-	3,14E-18	0,01	0,00	1946
		1935-02B	349,51180	0,01505	2,96916	0,00517	348,90060	99,6	7,43E-14	0,20	1264,96	4,68
		1935-02C	362,32610	0,01251	0,32461	0,00044	362,29990	100,0	2,63E-13	0,35	1299,54	2,56
		1935-02D	365,69280	0,01187	0,42724	0,00050	365,68050	100,0	4,63E-13	2,99	1308,17	2,56
RAPA-45	muscovite	1936-01A	484,85200	0,01726	0,00000	0,52028	331,09130	68,3	1,73E-15	0,25	1217,94	98,68
		1936-01B	354,17910	0,01181	0,00000	0,00089	353,91490	99,9	3,92E-13	0,40	1277,98	2,34
		1936-01C	352,40720	0,01835	2,29093	0,00794	350,77120	99,4	2,69E-14	0,60	1269,83	7,66
		1936-01D	323,56630	0,06380	14,22558	0,05125	312,47350	95,7	3,89E-15	0,85	1167,44	30,23
		1936-01E	346,77670	0,02854	7,89865	0,01850	343,72080	98,6	1,17E-14	2,55	1251,41	12,89
		1936-02A	204,53690	0,37225	0,00000	0,70043	-2,39487	-1,2	2,30E-16	0,32	-12,63	523,92
		1936-02B	185,18260	0,50512	238,79020	0,32391	128,32260	58,3	2,36E-16	0,40	572,83	299,31

1936-02C	382,47880	0,04942	0,00000	0,02613	374,76320	98,0	3,59E-15	0,60	1331,13	48,20
1936-02D	358,59190	0,01256	0,14299	0,00122	358,27450	99,9	4,86E-13	2,99	1289,22	3,51

REFERENCES:

- Almeida, F. F. M. de, 1965, Geologia da Serra da Bodoquena (Mato Grosso): Boletim DNPM, Divisão de Geologia e Mineralogia, v. 219, p. 1-137.
- Almeida, F. F. M. de, 1967, Origem e Evolução da Plataforma Brasileira: Boletim DNPM, Divisão de Geologia e Mineralogia, v. 241, p. 1-36.
- Alvarenga, C. J. S., Moura, C. A. V., Gorayeb, P. S. S., Abreu, F. A. M., 2000, Paraguay and Araguaia Belts, *in* Cordani, U. G., Milani, E. J., Thomas Filho, A., Campos, D. A., editors, Tectonic Evolution of South America: Rio de Janeiro, 31^o International Geological Congress, p. 183-193.
- Alvarenga, C. J. S. and Saes, G. S., 1992, Estratigrafia e sedimentologia do Proterozóico Médio e Superior da região sudeste do Craton Amazônico: Revista Brasileira de Geociências, v. 22, n. 4, p. 493-499.
- Amaral, G., Cordani, U. G., Kawashita, K., Reynolds, J. H., 1966, Potassium-Argon dates of basaltic rocks from Southern Brazil: *Geochimica et Cosmochimica Acta*, v. 30, p. 159-89.
- Araújo, H. J. T., Santos Neto, A., Trindade, C. A. H., Pinto, J. C. A., Montalvão, R. M. G., Dourado, T. D. C., Palmeira, R. C. B., Tassinari, C.C.G., 1982, Folha SF.21 – Campo Grande: geologia, geomorfologia, pedologia, vegetação e uso potencial da terra, *in* Levantamento de Recursos Naturais: Rio de Janeiro, DNPM, Projeto RadamBrasil, v. 28, p. 416.
- Barron, C. N., 1969, Notes on the stratigraphy of Guyana: Geological Survey of British Guiana, Rec. 6, n. 2, p. 1-28.
- Bartholomew, M. J., Hatcher, Jr., R. D., 2009, The grenville orogenic cycle of southern laurentia: unraveling sutures, rifts, and shear zones as potential piercing points for Amazonia: *Journal of South American Earth Sciences*, (in press, 2009), doi: 10.1016/j.jsames.2009.08.007.
- Bettencourt, J. S., Leite Jr., W. B., Ruiz, A. S., Matos, R., Payolla, B. L., Tosdal, R. M., 2009, The Rondonian san Ignacio province in the SW Amazonian Craton: an overview: *Journal of South American Earth Sciences*, (in press, 2009), doi:10.1016/j.jsames.2009.08.006.
- Boger, S. D., Raetz, M., Giles, D., Etchart, E., Fanning, C. M., 2005, U-Pb age data from the Sunsas region of eastern Bolivia, evidence for the allochthonous origin of the Paragua Block: *Precambrian Research*, v. 139, p. 121-146.
- Boggiani, P. C., Fairchild, T. R., Coimbra, A. M., 1993, O Grupo Corumbá (Neoproterozóico – Cambriano) na região central da Serra da Bodoquena (Faixa Paraguai), Mato Grosso do Sul: *Revista Brasileira de Geociências*, v. 23, n. 3, p. 301-305.
- Campanha, G. A. C., Boggiani, P. C., Warren, L., Grohmann, C. H., Caceres, A. A., 2008, Possibilidade de uma nova faixa móvel brasileira no norte do Paraguai, *in* 44^o Congresso Brasileiro de Geologia, p. 33.
- Cardona, A., Cordani, U. G., Ruiz, J., Valencia, V. A., Armstrong, R., Chew, D., Nutman, A. P., Sanchez, A. W., 2009, U-Pb Zircon Geochronology and Nd Isotopic Signatures of the Pre-Mesozoic Metamorphic Basement of the Eastern Peruvian Andes: Growth and Provenance of a Late Neoproterozoic to Carboniferous Accretionary Orogen on the Northwest Margin of Gondwana: *The Journal of Geology*, v. 117, p. 285-305. DOI: 10.1086/597472.
- Cordani, U. G., Cardona, A., Jimenez, D. M., Liu, D., Nutman, A. P., 2005, Geochronology of Proterozoic basement inliers in the Colombian Andes: tectonic history of remnants of a

- fragmented Grenville Belt. Terrane Processes at the Margins of Gondwana: Journal of Geological Society of London Special Publication 246, p. 329-346.
- Cordani, U. G., D'Agrella-Filho, M. S., Trindade, R., Brito Neves, B. B., 2003, Tearing up Rodinia: Terra Nova, v. 15, p. 350-359.
- Cordani, U. G., Fraga, L. M., Reis, N., Tassinari, C. C. G., Brito Neves, B. B., 2009, On the origin and tectonic significance of the intra-plate events of Grenvillian-type age in South America: A discussion: Journal of South American Earth Sciences, (in press, 2009), doi:10.1016/j.jsames.2009.07.002.
- Cordani U. G., Tassinari, C. C. G., Rolim, D. R., 2005, The basement of the Rio Apa Craton in Mato Grosso do Sul (Brazil) and northern Paraguay: a geochronological correlation with the tectonic provinces of the south-western Amazonian Craton: Gondwana, v. 12, p. 112.
- Cordani, U. G., Tassinari, C. C. G., Teixeira, W., Coutinho, J. M. V., 2008, U-Pb SHRIMP zircon ages for the Rio Apa Cratonic Fragment in Mato Grosso do Sul (Brazil) and northern Paraguay: tectonic implications, VI South American Symposium on Isotope Geology: San Carlos de Bariloche, Argentina, p. 1-8.
- Cordani, U. G., Tassinari, C. C. G., Teixeira, W., Coutinho, J. M. V., 2008b, The basement of the Rio Apa Craton in Mato Grosso do Sul (Brazil) and northern Paraguay: Tectonic implications and correlations, 33rd International Geological Congress, AMS-07 Crustal evolution of the cratonic nuclei of South America: Oslo, CD-ROM.
- Cordani, U. G. and Teixeira, W., 2007, Proterozoic accretionary belts in the Amazonian Craton, in Hatcher, R. D. Jr., Carlson, M. P., McBride, J. H., Martinez-Catalan, J. R., editors, 4-D Framework of Continental Crust: Boulder, Colorado, Geological Society of America Memoir 200, p. 297-320.
- Cordani, U. G., Teixeira, W., D'Agrella-Filho, M. S., Trindade, R. I., 2009, The position of the Amazonian Craton in supercontinents: Gondwana Research, v. 15, p. 396-407.
- Corrêa, J. A., Neto, C., Correia Filho, F. C. L., Scislewski, G., Cavallon, L. A., Cerqueira, N. L. S., Nogueira, V. L., 1976, Projeto Bodoquena: Goiânia, CPRM, 8 v. (Relatório final).
- Del'Arco, J. O., Silva, R. H., Tarapanoft, I., Freire, F. A., Pereira, L. G. M., Sousa, S. L., Luz, D. S., Palmeira, R. C. B., Tassinari, C. C., 1982, Geologia, in BRASIL, Levantamento de Recursos Naturais, 27, Folha SE.21 Corumbá e parte da Folha SE.20: geologia, geomorfologia, pedologia, vegetação e uso potencial da terra: Rio de Janeiro, Departamento Nacional da Produção Mineral, Projeto RadamBrasil, p. 25-160.
- Delgado, I. M., Souza, J. D., Silva, L. C., Silveira Filho, N. C., Santos, R. A., Pedreira, A. J., Guimarães, J. T., Angelim, L. A. A., Vasconcelos, A. M., Gomes, I. P., Lacerda Filho, J. V., Valente, C. R., Perrotta, M. M., Heineck, C. A., 2003, Província Tocantins, in Bizzi, L. A., Schobbenhaus, C., Vidotti, R. M., Gonçalves, J. H., editors, Geologia, Tectônica e Recursos Minerais do Brasil: Rio de Janeiro, CPRM, p. 281-292.
- DePaolo, D. J., 1981, A neodymium and strontium isotopic study of Mesozoic calc-alkaline granitic batholiths of the Sierra Nevada and Peninsular Ranges, California: Journal Geophysical Research, v. 86, n. B11, p. 10470-10488.
- Godoi, H. O. (Org.), 1999, Programa Levantamentos Geológicos Básicos do Brasil (PLGB): Aguidauana, Folha SF.21-X-A: Estado do Mato Grosso do Sul: Brasília, CPRM, 72 p.
- Godoi, H. O., Martins, E. G., Mello, J. C. R., 1999, Programa de Levantamentos Geológicos Básicos do Brasil - PLGB: folha SE. 21-Y-D - Corumbá, Folha SF.21-V-B - Aldeia Tomázia, Folha SF.21-V-D - Porto Murinho, escala 1:250.000.

- Godoy, A. M., Manzano, J. C., Araújo, L. M. B. de, Silva, J. A. da, 2009, Contexto geológico-estrutural do Maciço Rio Apa, sul do Cráton Amazônico-MS, *in* Simpósio de Geologia do Sudeste, 11/Simpósio de Geologia de Minas Gerais, 15: São Pedro, SBG, p. 20.
- Gower, C. F. and Krogh, T. E., 2002, A U-Pb geochronological review of the Proterozoic history of the eastern Grenville Province: *Canadian Journal Earth Sciences*, v. 39, p. 795-829.
- Jimenez, D. M., Juliani, C., Cordani, U. G., 2006, P-T-t conditions of high-grade metamorphic rocks of the Garzon Massif, Andean basement, SE Colombia: *Journal of South American Earth Sciences*, v. 21, p. 322-336.
- Kroener, A. and Cordani, U. G., 2003, African, southern Indian and South American cratons were not part of the Rodinia supercontinent: evidence from field relationships and geochronology: *Tectonophysics*, v. 375, p. 325-352.
- Kroonenberg S. B., 1982, A Grenvillian Granulite Belt in the Colombian Andes and its Relation to the Guiana Shield: *Geologie en Mijnbouw*, v. 61, p. 325-333.
- Lacerda Filho, A. V., Abreu Filho, W., Valente, C. R., Oliveira, C. C., Albuquerque, M. C. (Org.), 2004, *Geologia e recursos minerais do Estado de Mato Grosso: texto dos mapas geológico e de recursos minerais do Estado de Mato Grosso*, CPRM, SICME-MT, escala 1:1.000.000.
- Li, Z. X., Bogdanova, S. V., Collins, A. S., Davidson, A., De Waele, B., Ernst, R. E., Fitzsimons, I. C. W., Fuck, R. A., Gladkochub, D. P., Jacobs, J., Karlstrom, K. E., Lu, S., Natapov, L. M., Pease, V., Pisarewsky, S. A., Thrane, K., Vernikovsky, V., 2008, Assembly, configuration, and break-up history of Rodinia: A synthesis: *Precambrian Research*, v. 160, p. 179-210.
- Litherland, M., Annel, R. N., Darbyshire, D. P. F., Fletcher, C. J. N., Hawkins, M. P., Klinck, B. A., Mitchell, W. I., O'Connor, E. A., Pitfield, P. E. J., Power, G., Webb, B. C., 1989, The Proterozoic of Eastern Bolivia and its relationship to the Andean Mobile Belt: *Precambrian Research*, v. 43, p. 157-174.
- Loewy, S. L., Connelly, J. N., Dalziel, I. W. D., 2004, An orphaned basement block: the Arequipa-Antofalla basement of the central Andean margin of South America: *Geological Society of America Bulletin*, v. 116, p. 171-87.
- Pimentel, M. M., Whitehouse, M. J., Viana, M. G., Fuck, R. A., Machado, N., 1997, The Mara Rosa arc in the Tocantins Province: further evidence for Neoproterozoic crustal accretion in central Brazil: *Precambrian Research*, v. 81, p. 299-310.
- Priem, H. N. A., Boelrijk, N. A. I. M., Hebeda, E. H., Verdurmen, E. A. Th., Verschure, R. H., 1971, Isotopic ages of the Trans-Amazonian acidic magmatism and the Nickerie Metamorphic Episode in the Precambrian Basement of Suriname, South America: *Geological Society American Bulletin*, v. 82, p. 1667-1680.
- Priem, H. N. A., Andriessen, P. A. M., Boelrijk, N.A.I.M., Hebeda, E. H., Huguett, A., Verdurmen, E. A. Th., Verschure, R. H., 1982, Geochronology of the Precambrian in the Amazonas Region of southeast Colombia (western Guiana Shield): *Geologie en Mijnbouw*, v. 61, p. 229-242.
- Ramos, V. A., 1988, Late Proterozoic – Early Paleozoic of South America: a collisional history: *Episodes*, v. 11, p. 168-174.
- Ramos, V. A., 2008, The basement of the Central Andes: the Arequipa and related terranes: *Annual Review of Earth and Planetary Sciences*, v. 36, p. 289-324.
- Ramos, V. A., 2009, Anatomy and global context of the Andes: Main geologic features and the Andean orogenic cycle, *in* Kay, S. M., Ramos, V. A., Dickinson, W. R., editors, *Backbone of*

- the Americas: Shallow Subduction, Plateau Uplift, and Ridge and Terrane Collision: Geological Society of America Memoir 204, p. 31–65, doi: 10.1130/2009.1204(02).
- Ruiz, A. S., Simões, L. S. A., Neves, B. B. B., 2005, Maciço Rio Apa: extremo meridional do Cráton Amazônico, *in* Simpósio Nacional de Estudos Tectônicos - SNET, 10: Curitiba, SBG, p. 301-304.
- Sadowski, G. R. and Bettencourt, J. S., 1996, Mesoproterozoic tectonic correlations between eastern Laurentia and western border of the Amazon Craton: *Precambrian Research*, v. 76, p. 213-227.
- Santos, J. O. S., Rizzotto, G. J., Mcnaughton, N. J., Matos, R., Hartmann, L. A., Chemale Jr., F., Potter, P. E., Quadros, M. L. E. S., 2008, Age and autochthonous evolution of Sunsás Orogen in West Amazon Craton based on mapping and U-Pb geochronology: *Precambrian Research*, v. 165, p. 120-152.
- Sato, K., Tassinari, C. C. G., Kawashita, K., Petronilho, L., 1995, O Método Geocronológico Sm-Nd no IG/USP e suas aplicações: *Anais da Academia Brasileira de Ciências*, v. 67, p. 313-336.
- Silva, E. L., ms, 1988, Geologia da região da Serra da Alegria, extremo sul do cráton Amazônico, município de Porto Murtinho – MS: Dissertação (Mestrado), Instituto de Geociências, Universidade de São Paulo, São Paulo, 147 p.
- Steiger, R. H., Jäger, E., 1977, Subcommittee on Geochronology convention on the use of decay constants in geo- and cosmochronology: *Earth Planetary Science Letters*, v. 36, p. 359-362.
- Tassinari, C. C. G., Cordani, U. G., Nutman, A. P., van Schmus, W. R., Bettencourt, J. S., Taylor, P. N., 1996, Geochronological systematics on basement rocks from the Rio Negro-Juruena Province (Amazonian Craton) and tectonic implications: *International Geology Review*, v. 38, p. 161-175.
- Tassinari, C. C. G., Medina, J., Pinto, M. S., 1996, Rb-Sr and Sm-Nd geochronology and isotope geochemistry of central Iberian metasedimentary rocks (Portugal): *Geologie en Mijnbouw*, v. 75, p. 69-79.
- Teixeira, W., Bettencourt, J. S., Girardi, V. A. V., Onoe, A. T., Sato, K., 2006, Mesoproterozoic mantle heterogeneity in SW Amazonian Craton: $^{40}\text{Ar}/^{39}\text{Ar}$ and Nd-Sr evidence from mafic-felsic rocks, *in* Hansji, E., Mertanen, S., Rämö, T., Vuollo, J. (orgs.), *Dyke Swarms - time markers of crustal evolution: Proceedings of the V International Dyke Conference: London*, Taylor and Francis Group, v. 1, p. 113-129.
- Teixeira, W., Geraldes, M. C., Matos, R., Ruiz, A. S., Saes, G., Vargas-Mattos, G., 2009, A review of the tectonic evolution of the Sunsás belt, SW portion of the Amazonian Craton: *Journal of South American Earth Sciences*, (in press, 2009), doi: 10.1016/j.jsames.2009.09.007.
- Tollo, R. P., Corriveau, L., McLelland, J., Bartholomew, M. J., 2004, Proterozoic tectonic evolution of the Grenville orogen in North America: An introduction: *Geological Society of America Memoir*, v. 197, p. 1-8.
- Vasconcelos, P. M., Onoe, A. T., Kawashita, K., Soares, A. J., Teixeira, W., 2002, $^{40}\text{Ar}/^{39}\text{Ar}$ geochronology at the Instituto de Geociências, USP: instrumentation, analytical procedures, and calibration: *Anais da Academia Brasileira de Ciências*, v. 74, n. 2, p. 297–342.
- Wiens, F., ms, 1986, Zur lithostratigraphischen, petrographischen und strukturellen Entwicklung des Rio-Apa Hochlandes, Nordost Paraguay: Dissertation, Geologisches Institut der

Technischen Universität Clausthal, Clausthal, 280 p. (Clausthaler Geowissenschaftliche Dissertation, 19).

Williams, I. S., 1998, U-Th-Pb geochronology by ion microprobe, *in* MccKibben, M. A., editor, Applications of Microanalytical Techniques to Understanding Mineralizing Processes, Economic Geologists Short Course, p. 1-35.

Zimmerman, U., 2005, Provenance studies of very low-to low-grade metasedimentary rocks of the Puncoviscana complex, northwest Argentina: Geological Society of London Special Publication 246, p. 381-416.

RIO APA – FIGURE CAPTIONS

Fig. 1. Geotectonic sketch of Central South America, where the Rio Apa Craton is seen as an allochthonous feature, which was attached to the Amazonian Craton in the process of agglutination of Gondwana (adapted from Kroener and Cordani (2003). 1 – Cratonic areas; 2 – Neoproterozoic tectonic provinces; 3 – Rondonian-San Ignacio belt; 4 – Central Goiás Massif; 5 – Sunsás belt; 6 – Phanerozoic sedimentary covers; 7 – Pampean magmatic arc.

Fig. 2. The Rio Apa cratonic fragment seen as a prolongation of the Amazonian Craton, in Neoproterozoic time. Adapted from Ruiz et al. (2005).

Fig. 3. Geologic map of the main area of exposure of the Rio Apa Craton, in SW Mato Grosso do Sul state (Brazil) and northeastern Paraguay, bounded to the east by the Paraguay-Araguaia belt. (For Brazil, adapted from Lacerda Filho et al., 2004; for Paraguay, adapted from Wiens, 1986). The location of samples with U-Pb SHRIMP zircon ages is indicated. See text for details.

Fig. 4A to H. Concordia diagrams, showing the analytical points for the U-Pb SHRIMP zircon analyses of rocks from the Rio Apa Craton.

Fig. 5. Location of samples from the Rio Apa Craton analysed by Rb-Sr and Sm-Nd whole-rock methods.

Fig. 6A to D. Rb-Sr reference-whole rock isochron diagrams for samples of the Rio Apa Craton.

Fig. 7. Sm-Nd correlation diagram for samples of the Rio Apa Craton.

Fig. 8. Neodymium isotopic evolution diagram against time for samples of the Rio Apa Craton in which the $\epsilon_{Nd(T)}$ values were calculated relative to the U-Pb ages of the respective samples.

Fig. 9. Location of samples from the Rio Apa Craton dated by K-Ar and $^{40}\text{Ar}/^{39}\text{Ar}$ methods. Green circles = Ar/Ar method; Red circles = K-Ar method; B = biotite; M = muscovite; H = hornblende.

Fig. 10A to C. $^{40}\text{Ar}/^{39}\text{Ar}$ step-heating spectra for mineral samples of the Rio Apa Craton. Duplicate or triplicate analyses, obtained in different crystals, are shown in the same diagram.

Fig. 11. General histogram for the age determinations obtained on rocks from the Rio Apa Craton. It includes the Sm-Nd T_{DM} model ages, the Rb-Sr model ages for Rb-rich samples, as well the K-Ar plus Ar-Ar ages.

Fig. 12. Western and Eastern tectonic blocks of the Rio Apa Craton, based on the geographical distribution of the Sm-Nd model ages and lithotectonic units.

Fig. 13. Geotectonic sketch map of South America at the Precambrian-Cambrian boundary. The tentative outline of allochthonous blocks with different size, possibly trapped during the collisions of Laurentia and Gondwana, is suggested, as well as the possible distribution of the Rondonian-San Ignacio and Sunsás tectonic domains, below the Phanerozoic sedimentary covers. Most nomenclature of key tectonic elements is included in the figure. TB = *Transbrasiliano Lineament*. Cratonic areas: AMAZ = Amazonian, SL = São Luiz, SF = São Francisco, PA = Paranapanema, LA = Luiz Alves, RPL = Rio de La Plata. Allochthonous terranes: AR = Arequipa, AN = Antofalla, PAT = Patagonia.

TABLE 1

Summary of the Precambrian geologic framework of the Rio Apa Craton. See text and Figure 3 for details. * Rb/Sr isochron age, see section Geochronological Results.

Unit	Main lithologies and exposure areas	Preferred age (U-Pb zircon)	Geologic correlations and tectonic inferences
Baía das Garças granitoid rocks	Slightly foliated granitoid rocks near Moraria and Baía das Garças	1730 Ma	Granitoid rocks intrusive into the Alto Tererê association
Caracol leucogranites	Foliated, biotite-poor, leucocratic orthogneisses (neaby Caracol and western Paso Bravo province)	1730 Ma	Strongly deformed, medium to high metamorphic grade orthogneiss (arc type affinity)
Amolar unit	Quartzites, medium-grade sericite-schists and metavolcanics, intruded by granitoid plutons (along Rio Apa river)	?	Strongly folded, low metamorphic grade supracrustal sequence
Alto Tererê association	Garnet-muscovite-biotite schists, subordinate muscovite-biotite gneisses with quartzitic intercalations	?	Medium- to high metamorphic grade metasediments and associated basic rocks
Serra da Alegria suite	Anorthosites, leucogabbros and melagabbros	1790 Ma	Cumulatic mafic complex intrusive into the Aluminador granitoid suite
Serra da Bocaina Group	Porphyritic rhyolites, dacites, pyroclastic rocks and volcanic breccias (east of Porto Murtinho)	1790 Ma	Slightly deformed, felsic volcanism
Alumiador granitoid suite	Pink to grey, fine to medium grained, isotropic syeno to monzogranitic rocks (serra do Alumiador)	1850 Ma	Slightly deformed felsic magmatism intrusive into the Rio Apa Complex (West)
Paso Bravo Province	Hornblende-biotite banded gneisses and migmatites intruded by granites (Colonia Felix Lopez, Paraguay)	1850 Ma*	Paleoproterozoic crystalline basement (Paraguay)
Rio Apa Complex (North and West)	Banded gneisses and migmatites, minor amphibolites	1940 Ma	Paleoproterozoic crystalline basement (Brazil)

TABLE 2

Rb-Sr whole rock analytical data. See Appendix 1 and text for details.

SAMPLE	ROCK TYPE AND TECTONIC UNIT	Rb	Sr	Rb⁸⁷/Sr⁸⁶	Sr⁸⁷/Sr⁸⁶	T(Ma)
		(ppm)	(ppm)			(0.705*)
RIO APA COMPLEX						
4036 EG 28	Biotite gneiss	145.2	77.2	5.51	0.8355	1650
578 EG 39	Biotite gneiss	105.4	457.1	0.67	0.7232	-
ALUMIADOR GRANITIC SUITE						
RA-57	Pink Granite	225.0	72.9	9.118	0.923401	1670
RA-60	Isotropic Granite	205.41	35.51	17.417	1.11996	1660
RA-76	Isotropic Granite	170.0	180.6	2.743	0.776069	-
RA-77	Isotropic Granite.	220.4	104.7	6.185	0.858910	1730
RA-78	Foliated Granitoid	354.60	19.54	60.26	2.21426	1740
RA-79	Pink, isotropic Granite	342.89	40.58	25.97	1.34147	1705
CSF 01	Granite	190.4	86.4	6.41	0.8555	1630
CSF 02	Granite	219.0	39.9	16.45	1.1030	1680
CSF 06	Granite	229.3	85.9	7.87	0.8959	1690
578 EG 61	Granophyre	210.5	63.6	9.77	0.9063	1440
578 EG 62	Granophyre	211.1	41.9	15.03	1.0250	1480
578 EG 103	Granite	380.6	24.7	49.19	1.7560	1490
4037 EG 37	Porphyritic Granite	237.0	53.9	13.10	1.0060	1600
SERRA DA BOCAINA VOLCANICS						

CSF 03	Quartz porphyre	98.6	82.1	3.50	0.7871	-
CSF 04	Volcanic breccia	113.8	72.3	4.60	0.8045	1510
EG 56	Rhyolite	139.9	82.1	4.99	0.8207	1615
CSF 05	Volcanic breccia	139.2	37.1	28.39	1.4160	1740
EG 146	Riolito	413.4	28.7	45.58	1.7480	1590
EG 01	Rhyolite	133.4	89.7	4.35	0.8097	1670
EG 66	Rhyoliteo	238.6	34.5	21.60	1.1510	1440

BAÍA DAS GARÇAS GRANITOID ROCKS

RA-34A	Pink Granite	325.9	51.0	19.262	1.138854	1570
RA-35A	Pink Granite	314.0	23.9	41.490	1.65382	1590
RA-35B	Aplitic Granite	281.4	24.6	35.748	1.54456	1630
RA-36A	Pink Granite	314.6	19.4	52.987	2.00105	1700
RA-36B	Pink Granite	387.3	22.1	57.754	2.10557	1690
RA-37A	Pink-grey Granite	331.6	50.3	19.924	1.163021	1600
RA-38	Grey Orthogneiss	212.6	315.5	1.959	0.754374	-
RA-39	Pink Aplitic Granite	249.7	22.1	35.487	1.56161	1680
RA-40	Granite	260.3	47.6	16.412	1.08913	1630
4007 EG 13	Biotite Granite	276.1	45.6	18.23	1.1150	1570
4007 EG 15	Gneiss	222.8	289.9	2.24	0.7600	-
4007 EG 121	Gneiss	207.8	190.2	3.18	0.7812	-
4036 EG 39	Gneiss	221.0	27.2	24.82	1,2780	1610
4036 EG 98	Gneiss	97.7	297,9	0.95	0.7285	-
EG 102	Granite	143.1	186.0	2.24	0.7572	-

CARACOL LEUCOCRATIC GNEISSES						
RA-43	Pink Granite	211.2	30.6	20.977	1.21575	1690
RA-81	Leucocratic Gneiss	220.1	14.6	48.698	1.88942	1690
RA-83	Leucocratic Gneiss	172.7	150.9	3.339	0.790197	-
RA-85	Leucocratic Gneiss	277.0	75.4	10.879	0.934362	-
558 EG 107	Granite	238.0	75.7	9.30	0.9340	1710
4007 EG 83	Monzonite	230.3	259.0	2.59	0.7722	-
EG 103	Granitic Gneiss	314.5	78.5	11.92	0.9932	1680
CSF 07	Granite	173.4	55.6	9.23	0.9306	1700
PASO BRAVO GRANITOID ROCKS						
RA-95	Granitoid Gneiss	201.5	77.6	7.654	0.897480	1750
RA-110	Pink Granite	187.5	128.2	4.280	0.817053	1820
RA-111	Pink thin grained granite	281.9	41.5	20.723	1.25208	1835
RA-112	Biotite, pink granite	345.8	35.9	29.918	1.44879	1730
RA-113	Pink Granite	269.5	28.3	29.647	1.48343	1825
RA-114	Porphyritic Granite	176.7	287.2	1.788	0.749466	-
RA-115	Porphyritic Granite	15.2	286.5	1.604	0.745798	1770

Obs. * reference initial ratio. See Annex I and text for details.

TABLE 3
Sm/Nd whole rock analytical data. See Appendix 1 and text for details.

Sample	Rock	Sm (ppm)	Nd (ppm)	¹⁴⁷ Sm / ¹⁴⁴ Nd	¹⁴³ Nd / ¹⁴⁴ Nd	f _{Sm/Nd}	T _{DM} Ga	ε _{Nd(t)} (U-Pb age)	U-Pb age (Ma)
RIO APA									
JV 15	Gneiss	8.860	51.35	0.1043	0.511224	- 0.47	2.53	-4.72	1940
JV 18	Gneiss	13.225	71.429	0.1119	0.511567	- 0.43	2.20	+0.09	1940
JV 23	Gneiss	4.54	18.793	0.1461	0.512037	- 0.26	2.26	+0.80	1940
JV 24	Gneiss	3.405	13.122	0.1569	0.512189	- 0.20	2.28	+1.09	1940
JV 30	Granite	3.245	19.633	0.9990	0.511414	- 0.49	2.17	+0.08	1940
JV 1D	Gneiss	5.011	31.76	0.0954	0.511047	-0.51	2.57	-5.97	1940
PASO BRAVO PROVINCE									
RA 111	Leuc gneiss	2.862	12.555	0.1379	0.511869	- 0.30	2.37	-1.13	1850
RA 114	Porph. granite	7.990	41.311	0.1170	0.511648	- 0.41	2.20	-0.50	1850
ALUMIADOR GRANITIC SUITE									
RA 57	Granite	23.384	109.424	0.1292	0.511650	- 0.34	2.53	-3.34	1850
RA 76	Granite	4.415	23.360	0.1143	0.511426	- 0.42	2.49	-4.20	1850
RA 78	Leuc. gneiss	1.526	9.329	0.0989	0.511152	- 0.50	2.53	-5.91	1850
JV 7	Granophyre	10.310	50.117	0.1243	0.511639	- 0.37	2.38	-2.86	1800
JV 7A	Granophyre	8.587	38.968	0.1332	0.511680	- 0.32	2.58	-4.11	1800
CARACOL LEUCOCRATIC GNEISSES									
RA 83	Leuc gneiss	7.341	38.704	0.1147	0.511600	-0.42	2.23	-1.94	1750
CC 15	Leuc gneiss	25.171	129.76	0.1173	0.511632	--0.40	2.22	-1.90	1750
BAÍA DAS GARÇAS GRANITOID ROCKS									
RA 34A	Leuc. gneiss	5.289	27.402	0.1167	0.511724	- 0.41	2.07	+0.03	1750
RA 35B	Granite	3.571	24.801	0.0871	0.511419	- 0.56	1.96	+0.69	1750

RA 35A	Leuc. gneiss	3.251	20.788	0.0946	0.511464	- 0.52	2.02	-0.11	1750
RA 36B	Granite	2.584	10.757	0.1452	0.511795	- 0.26	2.81	-4.95	1750
RA 37A	Leuc. gneiss	5.107	26.760	0.1154	0.511731	- 0.41	2.04	+0.46	1750
RA 38	Orthogneiss	5.757	33.074	0.1053	0.511582	- 0.46	2.06	-0.20	1750
RA 39	Leuc. gneiss	3.566	20.098	0.1073	0.511553	- 0.45	2.14	-1.21	1750
RA 40	Leuc. gneiss	8.710	43.074	0.1223	0.511831	- 0.38	2.02	+0.87	1750
RA 43	Granite	9.775	56.420	0.1048	0.511636	- 0.47	1.97	+0.97	1750
SERRA DA ALEGRIA MAGMATIC SUITE									
JV 8	Anorthosite	2.230	9.192	0.1468	0.511886	- 0.25	2.64	-3.21	1800
JV 9B	Anorthosite	2.180	9.586	0.1375	0.511792	- 0.30	2.50	-2.91	1800
JV 14	Anorthosite	0.680	3.330	0.1250	0.511573	- 0.36	2.50	-4.31	1800
SERRA DA BOCAINA VOLCANICS									
JV 4	Rhyodacite	11.917	63.139	0.1141	0.511561	- 0.42	2.26	-2.04-	1800

TABLE 4
K-Ar analytical data. See Appendix 1 and text for details.

Sample	Rock	Material	%K	⁴⁰Ar rad ccSTP/g x 10⁻⁶	% Atm ⁴⁰Ar	Age (Ma)
RA 75	Granite	Biotite	5.49	412.34	1.8	1314 ± 19
RA 38	Orthogneis	Biotite	6.43	497.15	1.2	1342 ± 20
RA 40	Granite	Biotite	6.16	462.95	1.8	1315 ± 20
4036/EG- 85	Amphibolite	Amphibole	0.205	16.31	7.3	1374 ± 64
4036/EG- 14	Amphibolite	Amphibole	0.995	71.02	2.5	1267 ± 25
4007/EG- 50	Muscovite schist	Muscovite	8.18	582.2	0.5	1265 ± 14
578/EG-79	Amphibolite	Amphibole	0.324	13.64	3.4	853 ± 58

TABLE 5
Ar-Ar analytical data. See Appendix 1 and text for details.

Sample	Mineral	Plateau age, Ma	Integrated age, Ma	Observations
RIO APA (NORTH)				
RA 22	Muscovite	1283 ± 3	1284 ± 2	
		1281 ± 2	1281 ± 3	
RA 23	Biotite	1272 ± 3	1242 ± 2	
		1271 ± 4	1260 ± 4	Small plateau
PASO BRAVO PROVINCE				
RA 88C	Amphibole	1292 ± 10	1321 ± 4	Small plateau, 2 steps
RA 93A	Amphibole	-	2015 ± 13	Excess argon
		-	1529 ± 6	Excess argon
RA 112	Biotite	1290 ± 4	1267 ± 2	
		1295 ± 5	1296 ± 5	
RA 114	Biotite	-	1265 ± 3	Irregular spectrum
		1308 ± 3	1292 ± 2	
		1303 ± 2	1287 ± 2	
		1299 ± 3	1286 ± 2	
ALUMIADOR SUITE				
RA 76	Biotite	1303 ± 4	1292 ± 2	
		1302 ± 3	1296 ± 2	
RA 62F	Biotite	1295 ± 3	1279 ± 2	
		-	1124 ± 2	Irregular spectrum
CARACOL GNEISS				
RA 83	Biotite	1132 ± 3	1104 ± 2	
		1098 ± 3	1098 ± 3	
		1079 ± 4	1089 ± 2	
BAÍA DAS GARÇAS GRANITOID ROCKS				
RA 37A	Biotite	1310 ± 3	1294 ± 2	
		1310 ± 3	1303 ± 2	
RA 38	Biotite	1308 ± 5	1303 ± 3	
		1304 ± 5	1301 ± 2	
ALTO TERERÊ ASSOCIATION				
RA 52	Muscovite	1295 ± 5	1294 ± 3	
		1288 ± 6	1288 ± 6	
RA 32	Muscovite	1300 ± 3	1302 ± 2	
		1299 ± 3	1297 ± 2	
RA 33	Muscovite	1300 ± 4	1300 ± 3	
		1298 ± 5	1297 ± 3	
RA 45	Muscovite	1289 ± 5	1288 ± 4	
		1277 ± 3	1276 ± 2	

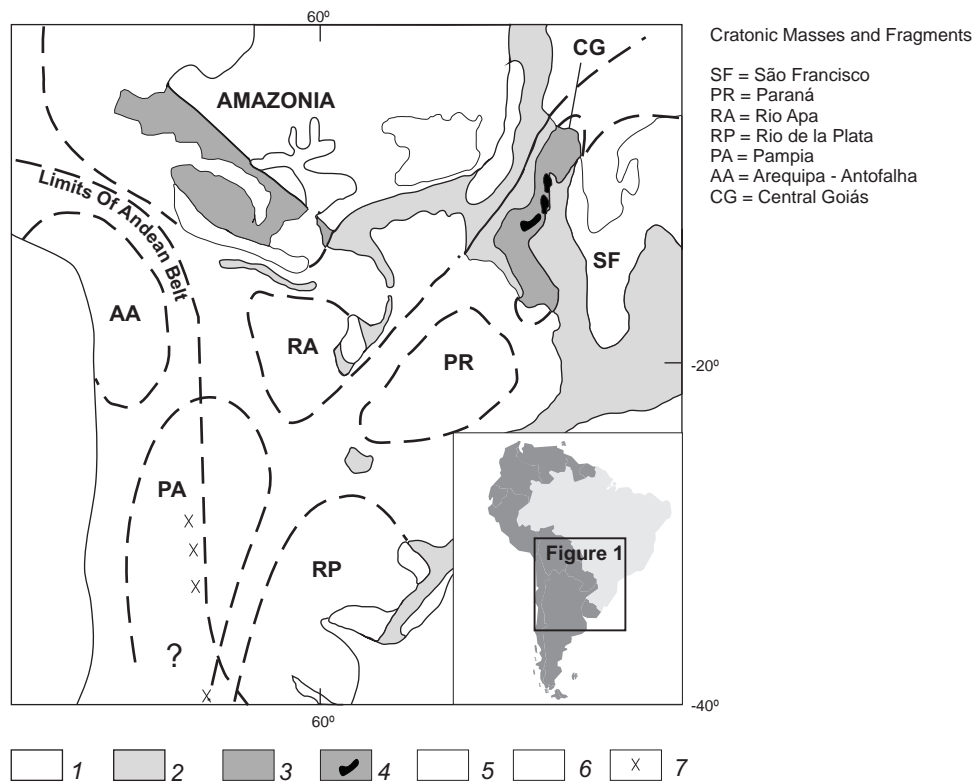


Fig. 1. Geotectonic sketch of Central South America, where the Rio Apa Craton is seen as an allochthonous feature, which was attached to the Amazonian Craton in the process of agglutination of Gondwana (adapted from Kroener and Cordani (2003)). 1 - Cratonic areas; 2 - Neoproterozoic tectonic provinces; 3 - Rondonian-San Ignacio belt; 4 - Central Goiás Massif; 5 - Sunsás belt; 6 - Phanerozoic sedimentary covers; 7 - Pampean magmatic arc.



Fig. 2. The Rio Apa cratonic fragment seen as a prolongation of the Amazonian Craton, in Neoproterozoic time. Adapted from Ruiz et al. (2005).

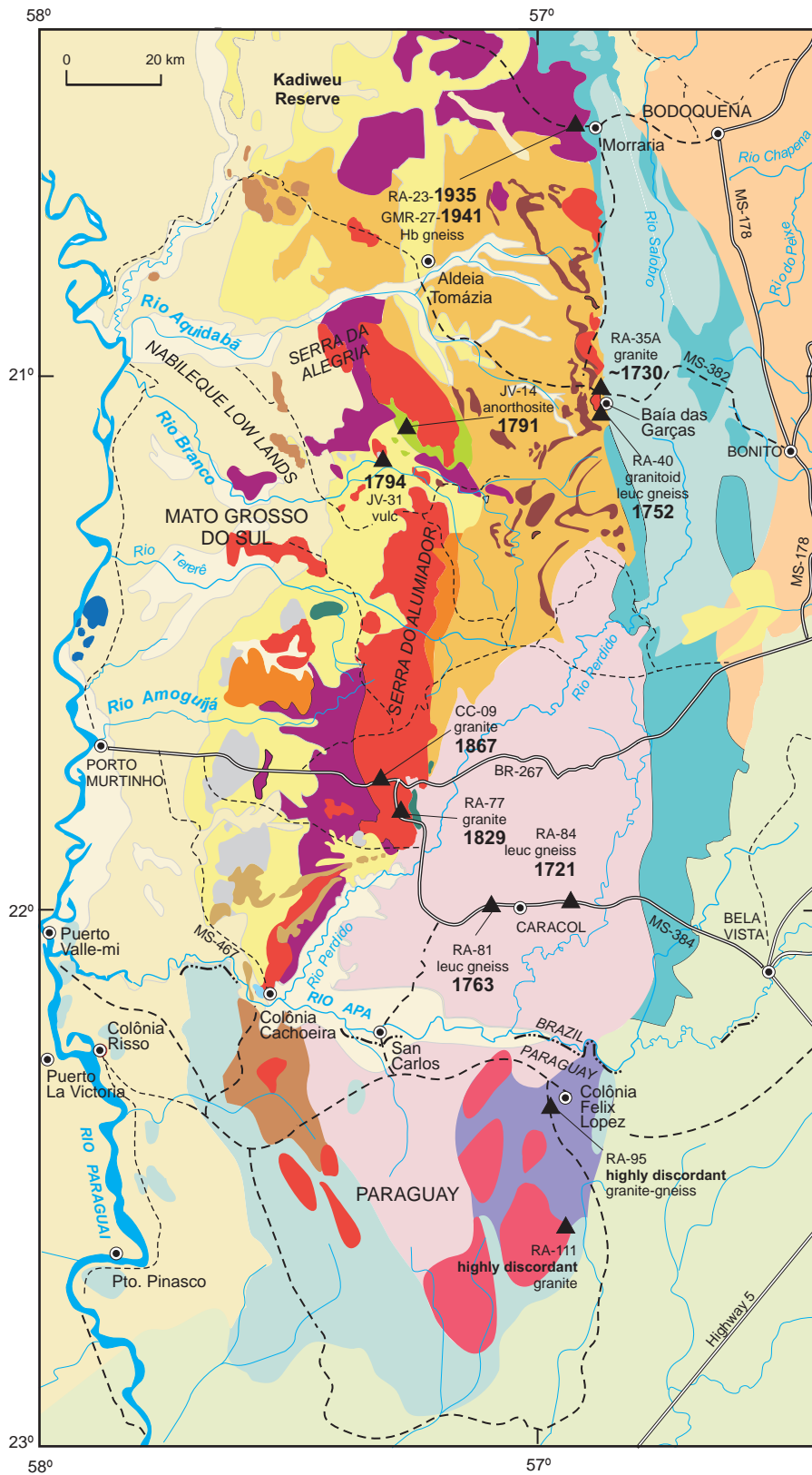


Fig. 3. Geologic map of the main area of exposure of the Rio Apa Craton, in SW Mato Grosso do Sul state (Brazil) and northeastern Paraguay, bounded to the east by the Paraguay-Araguaia belt. (For Brazil, adapted from Lacerda Filho et al., 2004; for Paraguay, adapted from Wins, 1986). The location of samples with U-Pb SHRIMP zircon ages is indicated. See text for details.

HOLOCENE


 Alluvium Deposits

PLEISTOCENE


 Alluvium Deposits

 Colluvium Deposits

TRIASSIC

 Fecho dos Morros Alkaline Suite

CARBONIFEROUS

 Aquidauana Formation

NEOPROTEROZOIC

Corumbá - Itapocumi Groups

 *Bocaina and Tamengo Formations*

 *Cercadinho Formation*

 Cuiabá Group


PALEOPROTEROZOIC


 Amolar Group

 Serra da Bocaina Formation

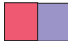
 Alumiador Granitic Complex (granites/ granophyres)

 Serra da Alegria Gabbro-anorthosite Suite

 Triunfo mafic Complex

 Alto Tererê low-medium grade metamorphics (schists and gneisses, granites, amphibolites)

 Caracol leucocratic gneisses

 Passo Bravo Province


 Rio Apa basement Complex

Fig. 3. Legend.

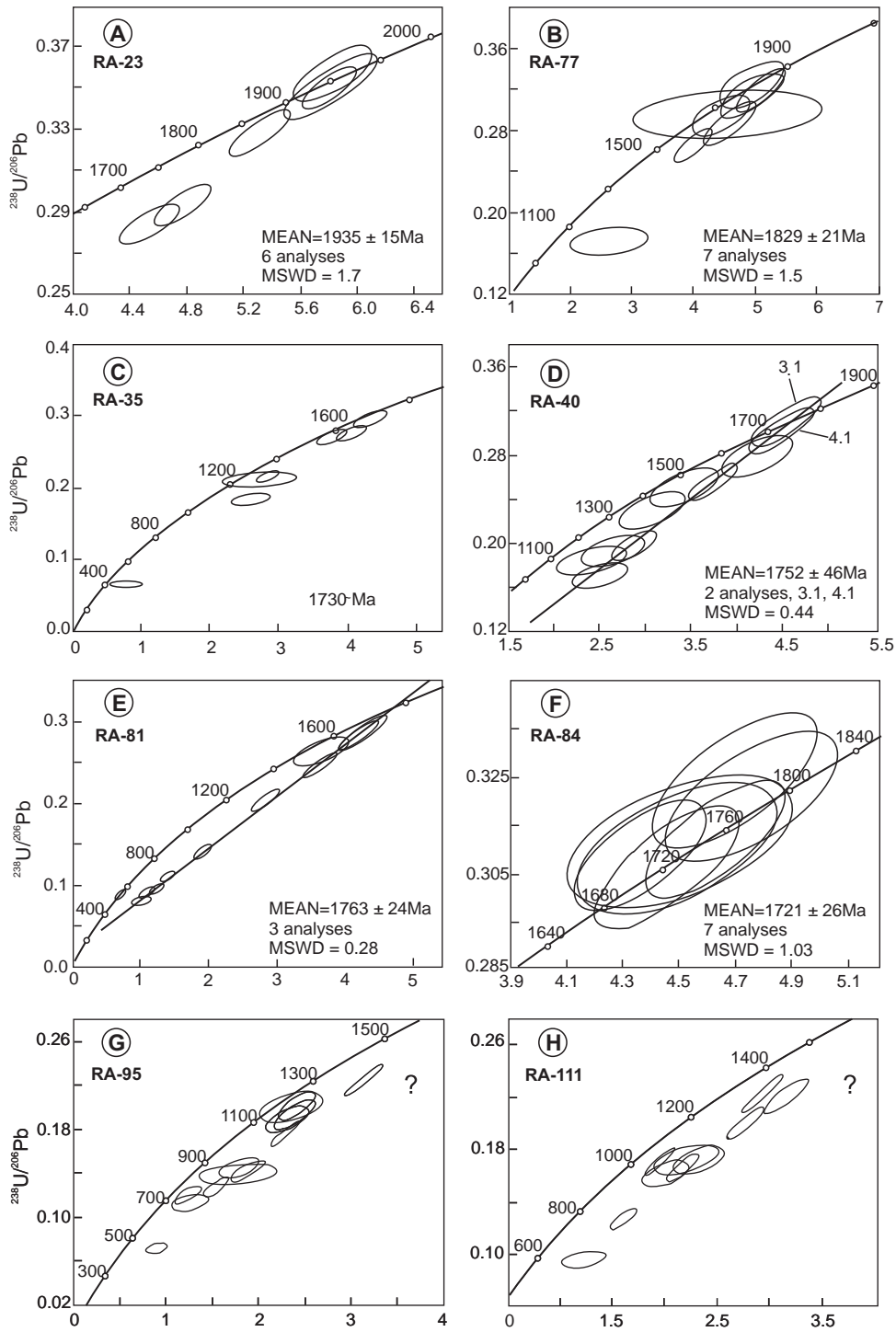


Fig. 4A to H. Concordia diagrams, showing the analytical points for the U-Pb SHRIMP zircon analyses of rocks from the Rio Apa Craton.

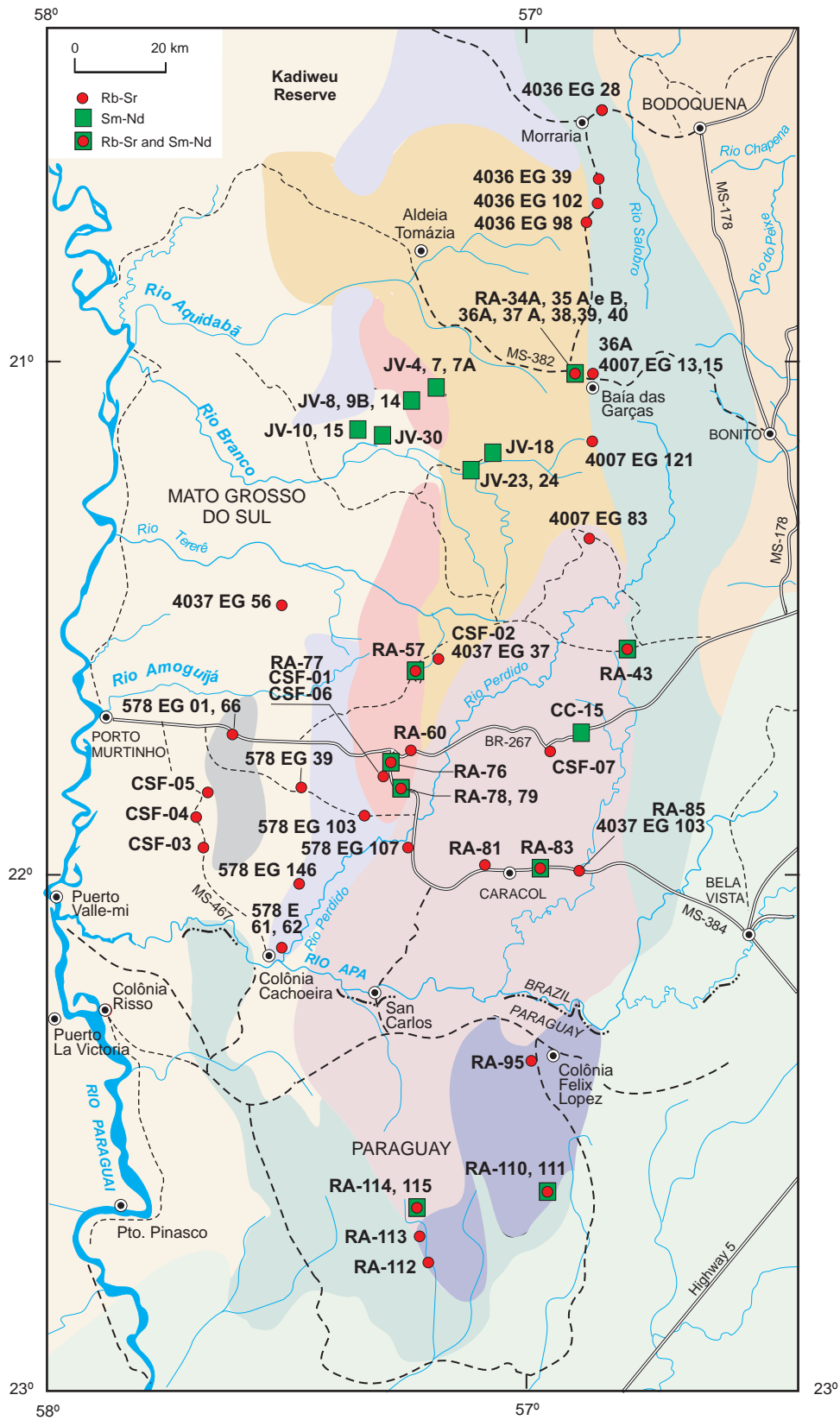


Fig. 5. Location of samples from the Rio Apa Craton analysed by Rb-Sr and Sm-Nd whole-rock methods.

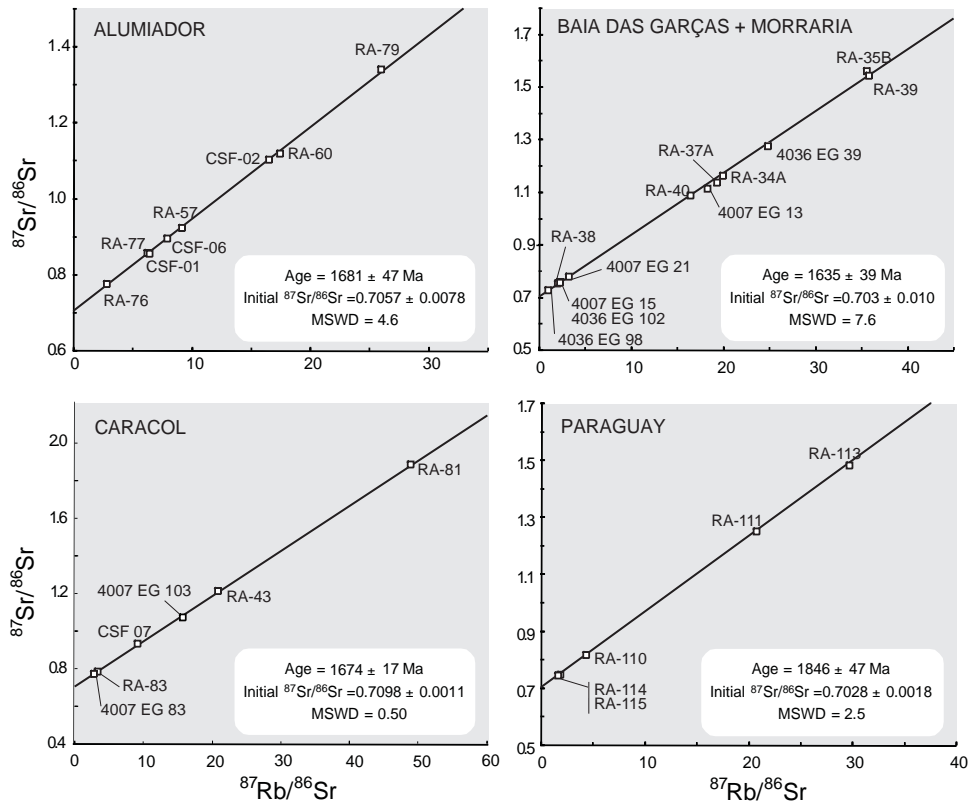


Fig. 6A to D. Rb-Sr reference-whole rock isochron diagrams for samples of the Rio Apa Craton.

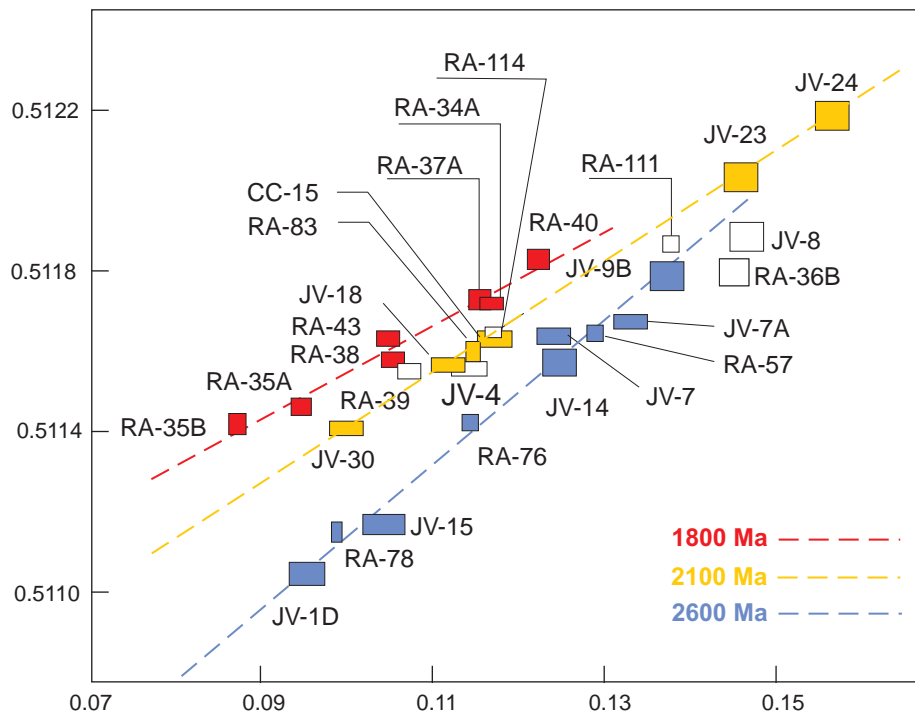


Fig. 7. Sm-Nd correlation diagram for samples of the Rio Apa Craton.

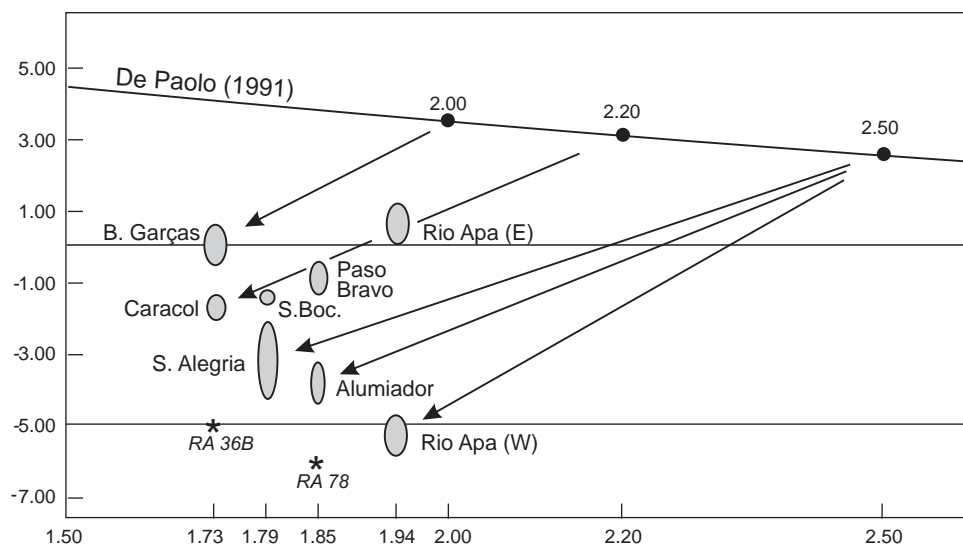


Fig. 8. Neodymium isotopic evolution diagram against time for samples of the Rio Apa Craton in which the $\epsilon_{Nd(T)}$ values were calculated relative to the U-Pb ages of the respective samples.

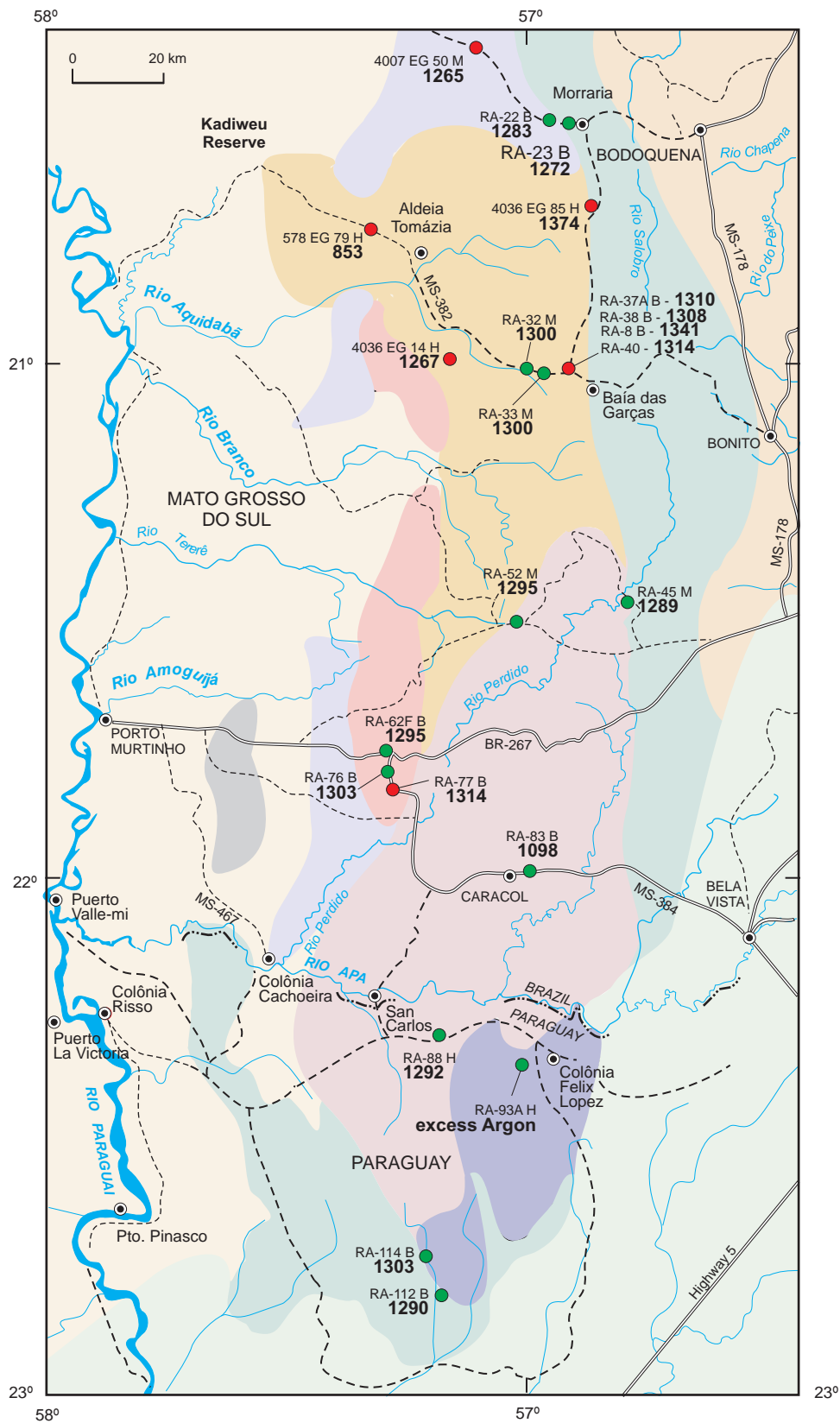


Fig. 9. Location of samples from the Rio Apa Craton dated by K-Ar and $^{40}\text{Ar}/^{39}\text{Ar}$ methods. Green circles = Ar/Ar method; Red circles = K-Ar method; B = biotite; M = muscovite; H = hornblende.

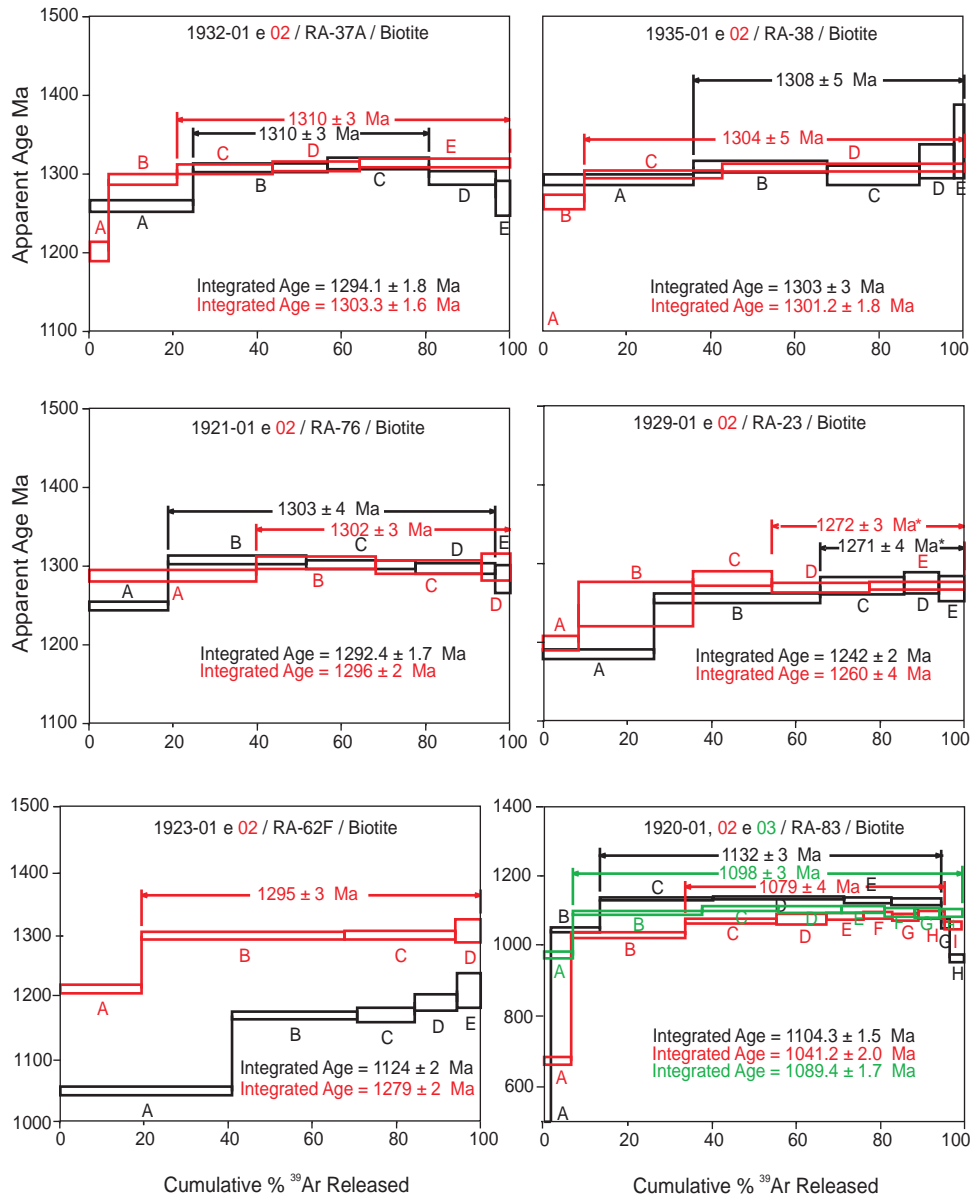


Fig. 10A to C. $^{40}\text{Ar}/^{39}\text{Ar}$ step-heating spectra for mineral samples of the Rio Apa Craton. Duplicate or triplicate analyses, obtained in different crystals, are shown in the same diagram.

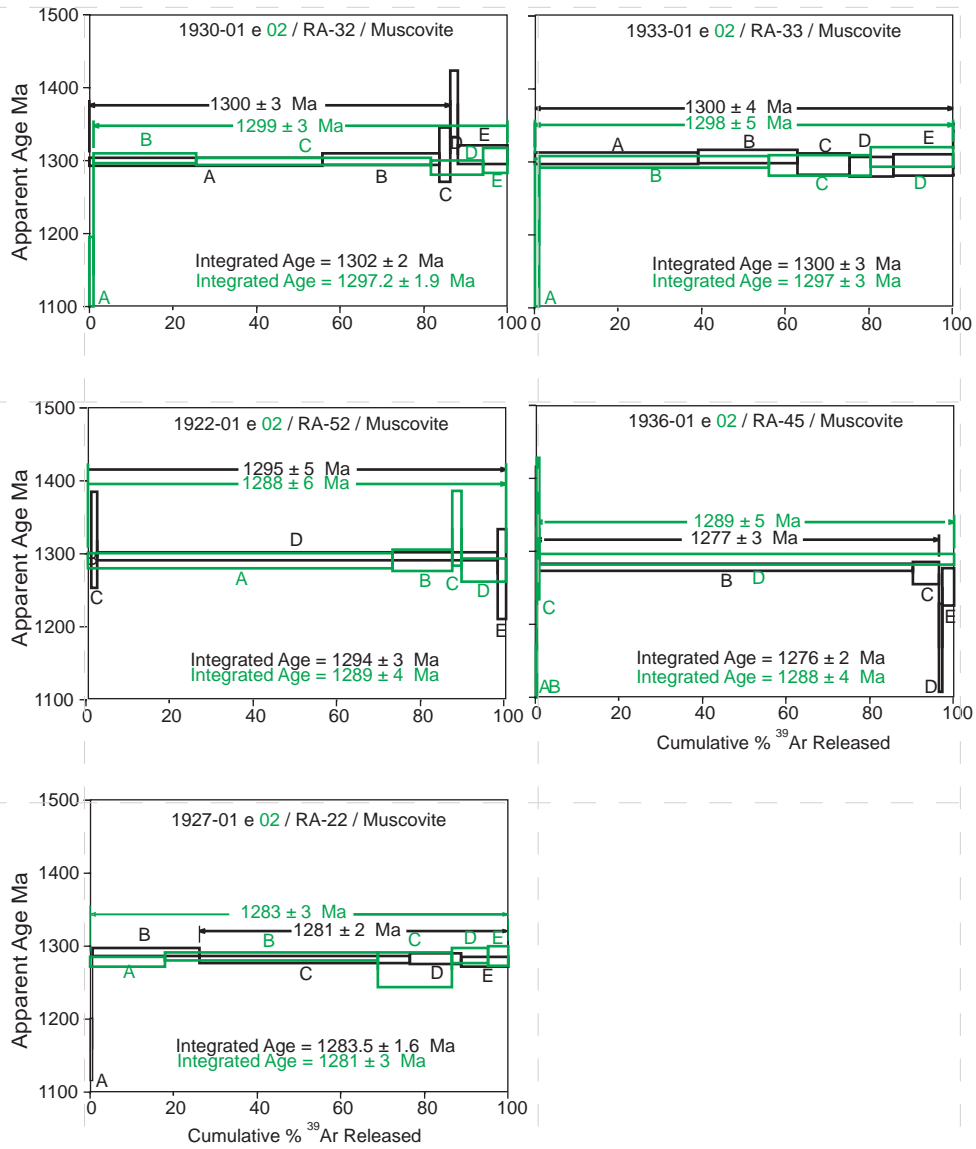


Fig. 10B.

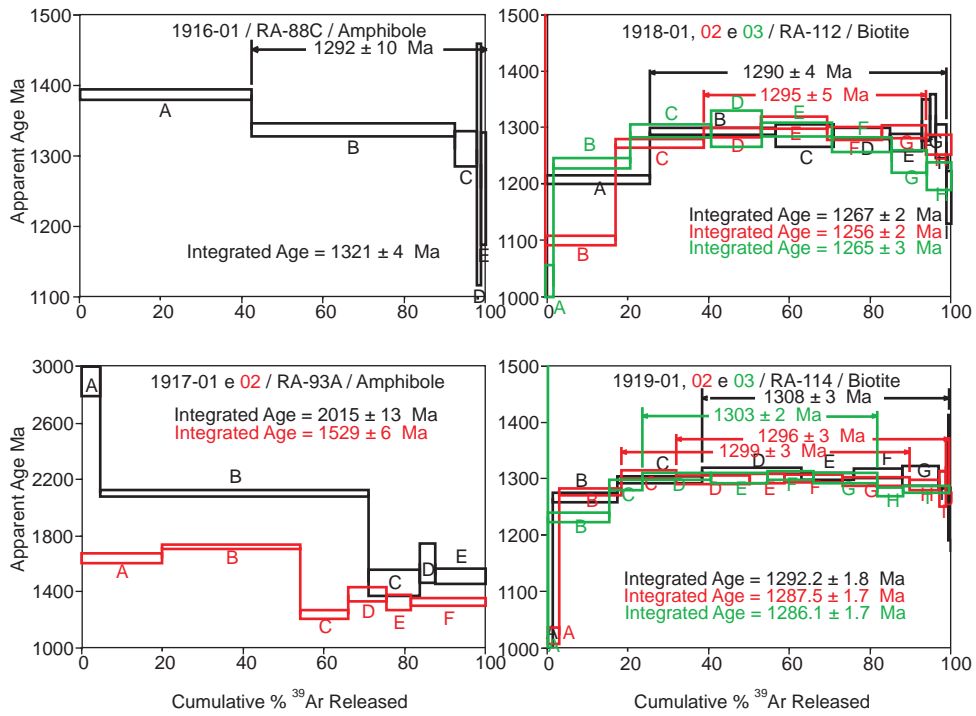


Fig. 10C.

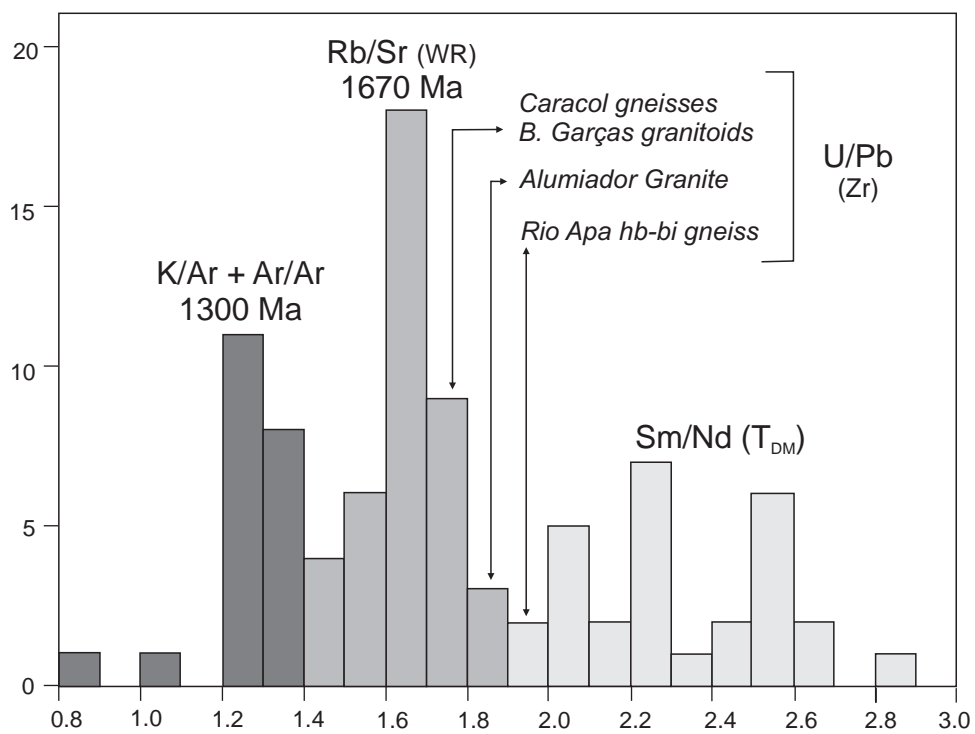


Fig. 11. General histogram for the age determinations obtained on rocks from the Rio Apa Craton. It includes the Sm-Nd T_{DM} model ages, the Rb-Sr model ages for Rb-rich samples, as well the K-Ar plus Ar-Ar ages.

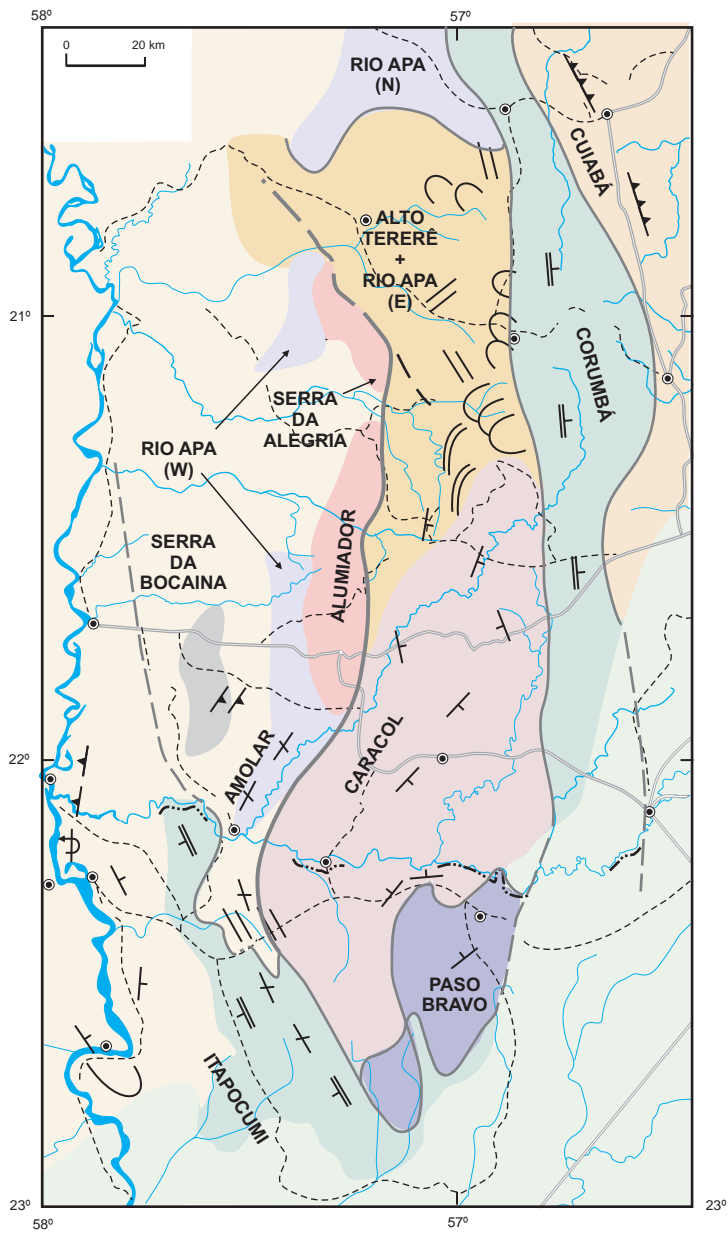


Fig. 12. Western and Eastern tectonic blocks of the Rio Apa Craton, based on the geographical distribution of the Sm-Nd model ages and lithotectonic units.

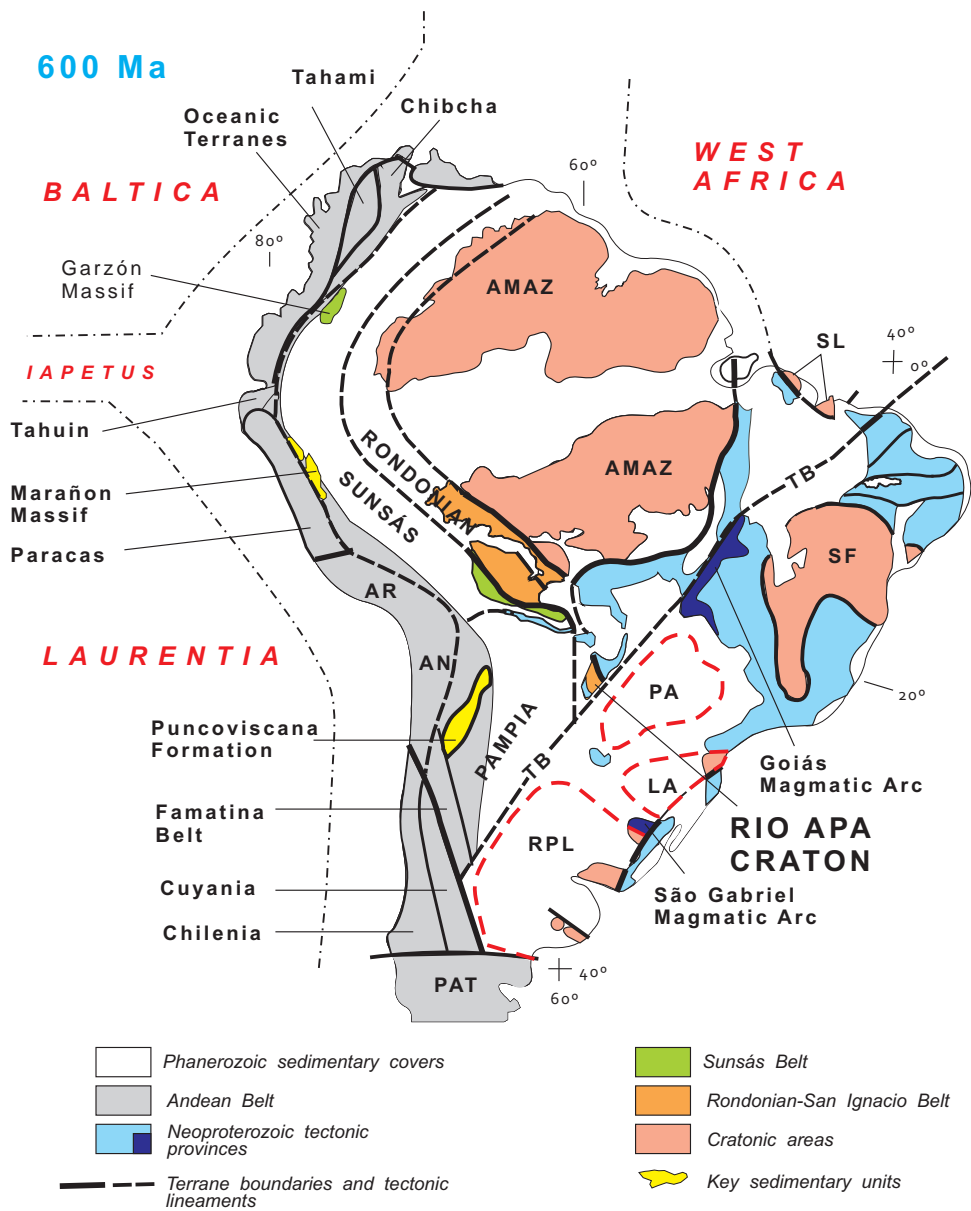


Fig. 13. Geotectonic sketch map of South America at the Precambrian-Cambrian boundary. The tentative outline of allochthonous blocks with different size, possibly trapped during the collisions of Laurentia and Gondwana, is suggested, as well as the possible distribution of the Rondonian-San Ignacio and Sunsás tectonic domains, below the Phanerozoic sedimentary covers. Most nomenclature of key tectonic elements is included in the figure. TB = *Transbrasiliano Lineament*. Cratonic areas: AMAZ = *Amazonian*, SL = *São Luiz*, SF = *São Francisco*, PA = *Paranapanema*, LA = *Luiz Alves*, RPL = *Rio de La Plata*. Allochthonous terranes: AR = *Arequipa*, AN = *Antofalla*, PAT = *Patagonia*.